



3 4456 0003112 3

ORNL/TM-9528

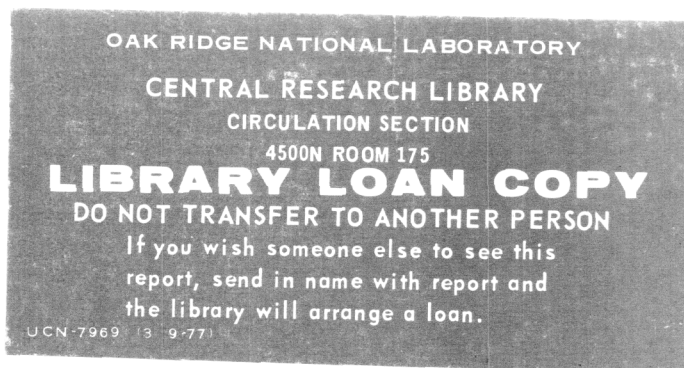
ornl

**OAK RIDGE
NATIONAL
LABORATORY**

MARTIN MARIETTA

Verification Experiment of the Three-Dimensional Oak Ridge Transport Code (TORT)

F. J. Muckenthaler
L. B. Holland
J. L. Hull
J. J. Manning



OPERATED BY
MARTIN MARIETTA ENERGY SYSTEMS, INC.
FOR THE UNITED STATES
DEPARTMENT OF ENERGY

Printed in the United States of America. Available from
National Technical Information Service
U.S. Department of Commerce
5285 Port Royal Road, Springfield, Virginia 22161
NTIS price codes—Printed Copy: A04 Microfiche A01

This report was prepared as an account of work sponsored by an agency of the United States Government. Neither the United States Government nor any agency thereof, nor any of their employees, makes any warranty, express or implied, or assumes any legal liability or responsibility for the accuracy, completeness, or usefulness of any information, apparatus, product, or process disclosed, or represents that its use would not infringe privately owned rights. Reference herein to any specific commercial product, process, or service by trade name, trademark, manufacturer, or otherwise, does not necessarily constitute or imply its endorsement, recommendation, or favoring by the United States Government or any agency thereof. The views and opinions of authors expressed herein do not necessarily state or reflect those of the United States Government or any agency thereof.

Engineering Physics and Mathematics Division

**VERIFICATION EXPERIMENT OF THE THREE-DIMENSIONAL
OAK RIDGE TRANSPORT CODE (TORT)**

F. J. Muckenthaler
L. B. Holland*
J. L. Hull*
J. J. Manning

Manuscript Completed: June 1985

Date Published: December 1985

*Operations Division

This Work Sponsored by
Defense Nuclear Agency
Under
Interagency Agreement No. 40-65-65

Prepared by the
OAK RIDGE NATIONAL LABORATORY
Oak Ridge, Tennessee 37831
operated by
MARTIN MARIETTA ENERGY SYSTEMS, INC.
for the
U.S. DEPARTMENT OF ENERGY
under Contract No. DE-AC05-84OR21400



3 4456 0003112 3

TABLE OF CONTENTS

Abstract	1
1. Introduction	1
2. Instrumentation	3
3. Experimental Configurations	4
3.1 Spectrum Modifier	5
3.2 SM + Block House + Concrete Window + Center Pillar	5
3.3 SM + Block House + Open Window + Center Pillar	6
3.4 SM + Block House + Open Window + Offset Pillar	6
3.5 SM + Block House + Open Window + Offset Pillar + Center Block Wall	6
4. Spectrum Modifier Measurements (Item I A)	7
5. Block House Measurements (Item II)	8
5.1 SM + Block House + Concrete Window + Center Pillar (Item II A)	8
5.2 SM + Block House + Open Window + Center Pillar (Item II B)	8
5.3 SM + Block House + Open Window + Offset Pillar (Item II C)	8
5.4 SM + Block House + Open Window + Offset Pillar + Central Block Wall (Item II D)	9
6. Discussion of Results	10
6.1 Bonner Ball Measurements	10
6.1.1 Measurements Beyond SM Without Block House	10
6.1.2 Bare Counter Measurements in Block House	10
6.1.3 Cd-Covered Counter Measurements in Block House	11
6.1.4 5-in. Bonner Ball Measurements in Block House	11
6.1.5 10-in. Bonner Ball Measurements in Block House	12
6.2 TLD Measurements	12
6.2.1 Measurements Beyond SM Without Block House	12
6.2.2 Measurements in Concrete Block House	13
7. Analysis of Experimental Errors	15
8. Conclusion	16
References	17
Acknowledgements	17
Appendix A. Program Plan for the Three-Dimensional Oak Ridge Transport Calculational Methods Verification Experiment	18
Appendix B. Tables of Data	20
Appendix C. List of Figures	42

VERIFICATION EXPERIMENT OF THE THREE-DIMENSIONAL OAK RIDGE TRANSPORT CODE (TORT)

ABSTRACT

An experiment was conducted at the Oak Ridge National Laboratory Tower Shielding Facility during FY 1984-85 to provide verification of a discrete ordinates Three-Dimensional Oak Ridge Transport computer code (TORT), which is being developed at ORNL for calculating the neutron and gamma-ray fluxes within concrete structures that were exposed to radiation at Hiroshima and Nagasaki. In the experiment a collimated beam of radiation from the Tower Shielding Reactor II, modified to represent the spectra of neutrons and gamma rays emitted in weapons bursts, impinged on a concrete structure simulating a small, simple, single-story concrete block house. Variations in the structure were introduced during the experiment by successive changes in the outer wall and within the building: several blocks in the front wall were removed to form a window; a concrete support pillar within the building was relocated; and a central concrete wall was added to divide the single room into two rooms of approximately the same dimensions. Integral neutron fluxes and gamma-ray energy depositions were measured both in the modified reactor beam and at selected locations inside each structure. This report describes the experiment and presents the detailed results in both tabular and graphical form. It also discusses the impact of the variations in the basic configuration on the measured results.

1. INTRODUCTION

During the latter part of FY 1984 an experiment was initiated at the Oak Ridge National Laboratory Tower Shielding Facility (ORNL TSF) to provide data for verification of the radiation transport computer code TORT¹ (Three Dimensional Oak Ridge Transport) under development at ORNL. This code is an extension of the two-dimensional discrete ordinates code DOT 4² to three-dimensional geometries. Developed as part of a continuing study supported by the Defense Nuclear Agency (DNA), TORT is being applied to calculations of the radiation that passed through walls, windows, and internal voids of large buildings that survived the explosive force of the atomic bombs at Hiroshima and Nagasaki. The experiment described in this report, also a part of the DNA study, attempted to simulate some of the exposures that possibly occurred during the detonations and to use the data for calculating the accuracy of the TORT code.

In the experiment, very simple structures, small by comparison to the actual structures being studied in the DNA program, were exposed to a collimated beam of radiation from the Tower Shielding Reactor II (TSR-II), and measurements were made of the radiations penetrating into the structures. So that

the spectra of neutrons and gamma rays in the reactor beam would more closely resemble the spectra of radiations emitted by "Little Boy," the bomb detonated over Hiroshima, the beam was altered by a "spectrum modifier" consisting of slabs of natural uranium (UO_2), borated polyethylene, and graphite (arranged in that order).

The basic experimental configuration (referred to as a "block house") was constructed of small concrete blocks and was 183 cm wide, 304.8 cm long, and 244 cm high. The front wall (the wall in the beam) and the back wall were solid, but both side walls contained two windows. A concrete pillar was located on the centerline of the structure.

As the experiment progressed, different structural features were mocked up by variations in the basic configuration. In the first change, concrete blocks were removed from the front wall to form a front window. This was followed by relocation of the concrete pillar and then the addition of a concrete wall that divided the single room into two rooms of similar dimensions.

The measurements made during the experiment consisted of integral neutron flux measurements made with the TSF Bonner ball detector system and gamma-ray energy absorption measurements made with CaF_2 thermoluminescent detectors. The measurements were made within the block house at positions that might have been occupied by individuals at the time the bomb exploded. Measurements were also made at various locations at the experimental site before the block house was placed in position. In addition, neutron flux measurements were made across the reactor beam at a position close to the spectrum modifier. This report describes the experiment and presents the detailed results in both tabular and graphical form. It also discusses the impact of the variations in the basic configuration on the measured results.

2. INSTRUMENTATION

The TSF Bonner ball detection system consists of a series of detectors (balls), each of which measures an integral of the neutron flux weighted by the energy-dependent response function for that ball. The detection device of a Bonner ball consists of a 5.1-cm-diameter spherical proportional counter filled with BF_3 gas ($^{10}\text{B}/\text{B}$ concentration = 0.96) to a pressure of 0.5 atmospheres. In order to cover a range of neutron energies, the counter is used bare, covered with cadmium, or enclosed in various thicknesses of polyethylene shells surrounded by cadmium, each detector being identified by the diameter of its shell. Bonner ball experimental results are predicted analytically by folding a calculated neutron spectrum with the Bonner ball response functions determined by Maerker et al.¹ and by C. E. Burgart et al.²

The thermoluminescent detectors (TLDs) used for the gamma-ray deposition measurements consisted of $\text{CaF}_2:\text{Mn}$ chips purchased from the Harshaw Chemical Company. They were 0.3175 cm on a side and approximately 0.089 cm thick. The chips were enclosed in iron capsules both during their calibration and during the measurements. The iron capsule was designed to provide a thickness greater than the maximum path length of the electrons induced from the incident gamma rays. The response of the chips was calibrated by exposing them to a known dose rate using a ^{60}Co gamma-ray source. Proper calibration of the TLDs relates the energy deposition to the intensity of the radiation field at each TLD location.

The measurements for each detector were referenced to the reactor power (watts) using as a basis the data from two fission chambers positioned in the reactor shield along the reactor centerline. The response of these chambers as a function of reactor power level had been established previously through several calorimetric measurements of the heat generated in the reactor during a temperature equilibrium condition (heat-power run).

3. EXPERIMENTAL CONFIGURATIONS

The experimental program plan (Appendix A) called for a series of neutron and gamma-ray measurements to be made of the flux incident upon and passing through the inside of the simulated Japanese concrete building (the block house) seen on the right in Fig. 1. The walls of the building were made of concrete blocks stacked around a skeleton iron frame that acted as a guide and attachment support for the walls. The front and side walls, 30.5-cm-thick, consisted of two rows of blocks which were 15.2 cm (6 in.) on a side and 30.5 cm (12 in.) long and were stacked side by side in an overlapping fashion to minimize possible streaming paths. The rear wall, 61 cm thick, was composed of a single row of large 61-cm-square by 30.5-cm-thick concrete blocks. A concrete pad in the experimental area served as the flooring for the block house, and 30.5-cm-thick concrete slabs were placed atop the blocks as the roof. The structure enclosed a volume whose dimensions were 183 cm across the front, 304.8 cm along the side, and 244 cm high. The side walls ran parallel to and were equally spaced on each side the reactor beam centerline. Each side wall contained two windows that were open at all times. The outside surface of the front wall was coincident with a vertical plane that passed through a point (as measured along the reactor beam centerline) 609.6 cm (20 ft) from the center of the reactor. The reactor beam centerline had been previously established as a horizontal line passing through the reactor center at a height of 207 cm above the concrete pad. This line was parallel to and 85 cm directly above the centerline of the concrete building, which was 122 cm above the pad. That is, the vertical plane that included the centerline of the block house also included the centerline of the beam.

A 61-cm-square column of concrete blocks (the same type as formed the rear wall) was placed inside the building to simulate a structural support pillar found in a typical multistoried Japanese structure. The pillar was movable: for two series of measurements it was centered in the vertical midplane of the block house and for two other series it was placed to the right of vertical midplane. For the last series of measurements, a 15.2-cm-thick concrete block wall that ran parallel to the front wall was placed directly behind the pillar, thus dividing the one large room into two rooms nearly equal in size.

An analysis of the concrete blocks used for front and side walls and the center wall is given in Table 1. The analyses of the concrete blocks used for the pillar and back wall and that for the concrete slabs in the ceiling are given in Tables 2A and 2B respectively. The analysis of the iron frame composition is given in Table 3. (Note: All tables are included in Appendix B.)

The TSR-II beam collimator covered by the spectrum modifier (SM) is shown at the left in Fig. 1. As noted in Section 1, the emerging spectrum of neutrons and gamma rays closely resembles the radiation profile from the "Little Boy" bomb exploded over Hiroshima. Preanalysis calculations³ fixed the composition and thickness of the spectrum modifier (SM) as described below.

3.1 SPECTRUM MODIFIER

The preanalysis calculations indicated that 20.3 cm (8 in.) of a UO_2 "radial blanket" (so named from its use in previous experiments at the TSF) followed by 10.2 cm (4 in.) of borated polyethylene and 15.2 cm (6 in.) of graphite (in that order) placed in the TSR-II beam as shown in Fig. 2 would alter the TSR-II spectra to be representative of the spectra estimated to have occurred at 500 m ground range from the Little Boy weapon. The radial blanket consisted of natural UO_2 pellets, 1.397 cm in diameter, stacked one on top of another to form rods that were enclosed in aluminum cylinders having a 1.524-cm outside diameter (see top view in Fig. 3). A 0.00508- to 0.01016-cm-thick void between the aluminum and the pellets was filled with argon. The aluminum cylinders were positioned vertically in an iron vessel in a triangular pitch of 1.608 cm, with the void between cylinders being filled with sodium. The iron-walled container had a designed thickness of 11.05 cm and a length of 152.4 cm on each side. Each of the two radial blankets (UO_2 slabs) used in this experiment contained 522 rods amounting to 64.6% of the volume of the slab. The rods were placed in seven rows with 74 and 75 rods per alternate row. The UO_2 density was 10.28 g/cc, 94% of the theoretical density. The aluminum cladding comprised 11.2% of the slab and the sodium comprised 23.2%, which left a void volume between the pellet and the aluminum cylinder of 1%. The pellet stack length in each of the rods was approximately 121.9 cm. These pellets were fabricated by Numes Corporation in 1962 to conform, in general, to the then AEC/RDT design standards for the Fast Flux Test Facility. Analyses of the UO_2 , sodium, and aluminum are given in Tables 4, 5, and 6, respectively.

The borated polyethylene slabs were 5.1 cm thick and 152.4 cm on a side. The composition of the borated slabs supplied by the vendor is given in Table 7. The graphite slab was 15.2 cm thick and was also 152.4 cm on a side. An analysis of the impurities of the slab is given in Table 8. The SM was surrounded on its lateral sides by 122 cm of concrete to minimize the amount of background radiation reaching the detector. This concrete shield, shown schematically in Fig. 2, was constructed of the 61-cm-square blocks whose composition is given in Table 2.

3.2 SM + BLOCK HOUSE + CONCRETE WINDOW + CENTER PILLAR

The concrete block house described above was positioned so that its front wall was perpendicular to the SM centerline at a point 609.6 cm (20 ft) from the center of the reactor (see Fig. 2). At this location the front wall was approximately 470 cm from the SM. As noted earlier, the centerline of the house was 122 cm above the pad and ran parallel to but 85 cm directly below the reactor beam centerline. Thus, radiation from the center of the reactor struck the center of the front face of the block wall at an angle of 8.06 degrees above horizontal with respect to the house centerline (81.94 degrees with respect to the front wall).

For the first block house configuration, the front wall was without a window as shown in Fig. 2. The windows in the sides of the house were open throughout the experiment. The 61-cm-square pillar of concrete was placed midway between the sides of the house, with its back face (the side opposite the reactor) centered midway along the length of the house.

3.3 SM + BLOCK HOUSE + OPEN WINDOW + CENTER PILLAR

For the second block house configuration, concrete blocks were removed from the front wall to form a window. This provided a 61×122 cm opening, the same as the side windows. This arrangement is shown in Fig. 4 and a photograph of it appears in Fig. 5.

3.4 SM + BLOCK HOUSE + OPEN WINDOW + OFFSET PILLAR

In the third configuration, shown in Fig. 6, the 61-cm-square pillar was relocated so that it resided adjacent to the iron framework on the right side of centerline, leaving a 7.62-cm-thick void between it and the wall. The inside face of the pillar was 22.9 cm from the centerline of the house.

3.5 SM + BLOCK HOUSE + OPEN WINDOW + OFFSET PILLAR + CENTER BLOCK WALL

In the final configuration, the pillar remained offset and a 15.2-cm-thick concrete block wall was placed across the width of the house directly behind the concrete pillar. This building arrangement is shown in Fig. 7.

4. SPECTRUM MODIFIER MEASUREMENTS (ITEM I A)

Data for verification of the neutron source term calculations were provided by a series of horizontal traverses with the bare and Cd-covered BF_3 counters and the 5- and 10-in.-diam Bonner balls made at several locations within the experimental area *before* the block house was placed in position. The first measurements were 30 cm beyond the SM and in its horizontal midplane (207 cm above the concrete pad). The results for these traverses are given in Table 9.

Similar horizontal traverses were made at three additional heights above the concrete pad (275, 205, and 91 cm) prior to installation of the block house. These traverses were within a vertical plane that was 470 cm beyond the SM [or 609.6 cm (20 ft) from the vertical axis of the reactor] and perpendicular to the centerline of the SM. This vertical plane coincided with the front face of the concrete block house when it was placed in position. The data from these traverses are given in Tables 10 through 12. As noted above, the horizontal midplane of the reactor beam was at a height of 207 cm; thus the traverse at the 205-cm height closely approached the beam centerline.

Bonner ball traverses were also made along the line 122 cm above the concrete pad that corresponded to the centerline of the block house when it was in position. These traverses began at the 470-cm reference point noted earlier (470 cm from the SM, 20 ft from the vertical axis of the reactor) and extended 390 cm into the region to be occupied by the block house (to a distance of 860 cm from the SM). These data are presented in Table 13 (see "foreground + background" count rates).

An attempt was made to also measure the neutron fluxes reaching the Bonner ball detectors from sources other than the face of the SM. For measurements of these "background" fluxes, two slabs of lithium hydride (LiH), each 30.5 cm thick and 152.4 cm on a side, were positioned against the SM to absorb neutrons in the beam. Horizontal traverses were then made with all four detectors at the 122-cm height in the vertical plane 470 cm from the SM. The results are given in Table 14. Background measurements were also taken at two points along the line corresponding to the centerline of the block house, and these results are included in Table 13.

Data for verification of the gamma-ray source term calculations were obtained with TLDs exposed in the same vertical plane described above, that is, the plane 470 cm from the SM that would include the front face of the block house. These measurements were made along horizontal lines 106, 206, and 275 cm above the concrete pad at locations that were in the vertical midplane of the reactor beam and 76.2 and 152.4 cm to each side of the vertical midplane (see Fig. 8). Four TLD measurements were also made at the 122-cm height along the line corresponding to the centerline of the block house. These measurements were made at 122-cm intervals, the first measurement being in the vertical plane 470 cm from the SM. These results are listed in Tables 15A and B respectively.

5. BLOCK HOUSE MEASUREMENTS (ITEM II)

5.1 SM + BLOCK HOUSE + CONCRETE WINDOW + CENTER PILLAR (ITEM II A)

Bonner ball traverses with the bare and Cd-covered BF_3 counters and the 5- and 10-in. Bonner balls were made in the horizontal midplane of the block house (122 cm above the concrete pad) both 61 cm beyond the front wall and 61 cm in front of the back wall as shown in the top view of Fig. 9. The results of the measurements 61 cm beyond the front wall are given in Table 16 and in Figs. 10 through 13, and those 61 cm in front of the back wall are presented in Table 17 and Figs. 14 through 17.

TLD exposures were also made in the horizontal midplane of the block house, as well as at points above and below the horizontal midplane. The measurements in the horizontal midplane were made along the centerline at distances of 15.2, 76.2, 167.7, and 289.6 cm from the front wall (see points 2, 4, 7, and 11 in Fig. 9) and at locations 61 cm from the centerline at these same distances (see points 1, 3, 5, 9, 10, and 12). Points 6 and 8 in Fig. 9 identify the locations of TLD measurements 91.4 cm below and 91.4 cm above the centerline point at the 167.6-cm distance. These energy deposition measurements are given in Table 18 and, except for the two locations above and below the horizontal midplane, the values are plotted in Fig. 18.

5.2 SM + BLOCK HOUSE + OPEN WINDOW + CENTER PILLAR (ITEM II B)

Neutron flux and TLD measurements were made for this configuration at the same locations in the block house as those described in Section 5.1 (see Fig. 9). Data from the Bonner ball traverses 61 cm beyond the front wall are given in Table 19 and are compared with the Item II A data in Figs. 10 through 13. Data from the traverses 61 cm in front of the back wall are presented in Table 20 and compared with the Item II A data in Figs. 14 through 17. The results from the TLD exposures are included in Table 18 and Fig. 18.

5.3 SM + BLOCK HOUSE + OPEN WINDOW + OFFSET PILLAR (ITEM II C)

The Bonner ball traverses for this configuration also were made at the same locations in the block house as those for the two previous configurations (see Fig. 9). The data from the traverses 61 cm beyond the front wall are given in Table 21 and in Figs. 10 through 13, and the data from the traverses 61 cm in front of the back wall are presented in Table 22 and in Figs. 14 through 17.

For this configuration the positions for the TLD measurements were reduced in number from 12 to 10, with no exposures made at the locations above and below the centerline point at the 167.6-cm distance. The results from these measurements are included in Table 18 and Fig. 18.

5.4 SM + BLOCK HOUSE + OPEN WINDOW + OFFSET PILLAR + CENTRAL BLOCK WALL (ITEM II D)

For this final configuration, the Bonner ball measurements were once again repeated at the same locations and the TLD exposures were again made only in the horizontal midplane of the block house. The Bonner ball results for the traverse 61 cm beyond the front wall are given in Table 23 and Figs. 10 through 13, and those for the traverse 61 cm in front of the back wall are given in Table 24 and Figs. 14 through 17. The TLD results are included in Table 18 and Fig. 18.

6. DISCUSSION OF RESULTS

6.1 BONNER BALL MEASUREMENTS

6.1.1 Measurements Beyond SM Without Block House

The bare detector data from traverses 470 cm behind the SM, that is, within the vertical plane at which the front face of the block house was to be located, indicated a gradual decrease in the thermal-neutron flux as the detector was moved from a height of 91 cm to 205 cm and then to 275 cm above the pad (compare Tables 10-12). This is as would be expected, since the concrete pad would have been providing a source of scattered neutrons whose energies were below the Cd-cutoff region. The data obtained with the 5- and 10-in. Bonner balls were a bit different in that the count rates at a height of 91 cm were less than those at 205 cm but greater than those at 275 cm. The Cd-covered detector count rates were nearly the same at the 91- and 205-cm heights (agreement was to within 2% on centerline) but dropped about 10% at the 275-cm height. All these results show neutron scattering in the concrete pad did indeed introduce a new source of low-energy neutrons.

The background measurements made 122 cm above the pad with the bare BF_3 counter indicate that on centerline at this height the thermal-neutron flux contribution to the background would be less than 10% of the total thermal-neutron flux. Similarly, background measurements on centerline with the other three detectors indicate that the background should be less than 5% of the count rates at the three heights without the LiH present.

6.1.2 Bare Counter Measurements in Block House

The count rates from the horizontal traverses with the bare BF_3 counter at 61 cm beyond the front wall of the block house for the various mockups are plotted in Fig. 10 (see also Tables 16, 19, 21, and 23). The figure shows that with the solid concrete front wall (no window) there is a small rise in the flux as the centerline of the house is reached. Removal of the blocks to form an open window in the front wall increased the flux by a little more than a factor of two at the centerline but by only about 50% at the sides of the room. Moving the pillar to the right side of the room decreased the flux about 25% at the centerline, the decrease being indicative of the loss of the backscattering from the pillar. At the same time, there was a slight increase in flux at the right side with the movement of the pillar in that direction, causing a small asymmetry as seen in the curve profile. Adding the wall at the center of the room provided a large scattering surface which increased the flux about 35% left of centerline, about 25% at centerline, and even about 15% in front of the pillar.

For the traverses 61 cm in front of the back wall, the presence of the pillar in the middle of the house introduced a slight dip in the count rate near the centerline in the configuration with the solid

front wall (see Fig. 14). Opening the window in the front wall increased the count rates on each side of the pillar nearly a factor of two, but increased that behind the pillar by only about 50%. Moving the pillar to the right side increased the flux at the centerline by about a factor of two, causing a count rate peak to occur along the centerline, again introducing a small asymmetry in the curve as the increase in count rate to the right of the centerline was noticeably less than that to the left of the centerline. Adding the wall in the middle of the room reduced the count rate on centerline more than a factor of two, with slightly less change noted near the walls of the building.

6.1.3 Cd-Covered Counter Measurements in Block House

The curve for the Cd-covered detector traverse 61 cm beyond the solid front wall (see Fig. 11) shows essentially a flat count rate with just a slight rise at centerline. Creating the open window in front, however, increased the count rate better than a factor of five at centerline, with much less change, about 60%, at the side walls. Moving the pillar to the right side dropped the count rate at the centerline by about 20%; the decrease was about half that amount to the left of centerline and was even smaller in front of the pillar. When the center wall was added, the count rate increased about 10% on centerline, nearly 30% left of centerline as the outside wall was approached, and only slightly more than 10% at the right side in front of the pillar.

The count-rate curve for the Cd-covered detector traverse 61 cm in front of the back wall (see Fig. 15) was concave downward for the configuration with the solid front wall, dropping about 40% at centerline from that at the sides. Opening the front window still left a concave-sloped curve around the centerline, but the count rate peaked on each side of the pillar — by about a factor of 2.5 over the solid-wall count rate. The count rates were not equally intense on both sides of the pillar, however, suggesting either that the pillar was not exactly on centerline or the window-pillar alignment was not coincident with the SM centerline or a combination of both. Moving the pillar off centerline increased the flux on centerline another factor of about four, with the curve again askew because of the shielding from the pillar. Adding the wall across the middle eliminated the previously gained factor-of-four flux at centerline, with the curve being nearly flat except for a small dip behind the pillar.

6.1.4 5-in. Bonner Ball Measurements in Block House

As was the case for the Cd-covered detector, the traverse with the 5-in. Bonner ball 61 cm beyond the solid front wall (Fig. 12) resulted in a basically flat curve, again with just a slight rise in the middle. When the window was opened, the count rate peaked at the centerline with a count rate that was a factor of about six greater than that observed for the solid wall configuration. Near the side walls, however, the increases were only about 50%. Moving the pillar to the right decreased the centerline count rate about 15% due to loss of backscattering, while, as previously observed for the Cd-covered

detector, it enhanced the count rate on the right side of centerline. Adding the center wall to the configuration increased the flux at the centerline and in front of the pillar about 10%. The wall did not add much to the scattered component at these locations, but it did make a more significant contribution (about 30%) to the flux left of centerline.

Measurements with the 5-in. ball at the back of the room again indicated a depression in the flux at the centerline directly behind the pillar when the front wall was solid (see Fig. 16). With the front window open, the flux again peaked unequally on each side the pillar, as it had in the previous traverse. Moving the pillar to the right increased the flux on centerline by nearly a factor of six, and again the shape was similar to that with the Cd-covered detector. Placing the block wall in the middle of the room reduced the flux better than a factor of four on centerline, leaving only a slight rise in the flux there, while causing a small depression in the data behind the pillar.

6.1.5 10-in. Bonner Ball Measurements in Block House

When the traverses made with the 5-in. Bonner ball were repeated with the 10-in. Bonner ball, the results were similar. With the solid front wall, the count rate at 61 cm behind the wall gradually increased as the detector moved toward the centerline (see Fig. 13). Opening the front window increased the flux on centerline nearly a factor of seven over that obtained behind the solid wall, a factor slightly higher than that obtained with the 5-in. ball. Moving the pillar to the right dropped the centerline count rate about 10%, with less of a decrease occurring on the right side in front of the pillar than on the opposite side without the pillar. The presence of the wall in the middle of the room increased the count rate on centerline ever so slightly, maybe 4%, with a similar increase in flux in front of the pillar, while near the opposite wall (left side) the count rate increased about 20%.

The traverse in front of the back wall showed a larger depression in the flux behind the pillar than had been obtained with the other detectors when the front wall was solid (see Fig. 17). Inserting the window in the front wall again produced unequal peaks on each side of the pillar, with the count rate in the peak to the left of the pillar increasing nearly a factor of five. Even behind the pillar the count rate increased about 70%. Moving the pillar to the right side increased the flux on centerline about a factor of 10, with only about a 50% increase near the walls. Placing the block wall in the middle of the house dropped the count rate about a factor of four on centerline and less than a factor of two at the sides of the house.

6.2 TLD MEASUREMENTS

6.2.1 Measurements Beyond SM Without Block House

As described earlier, the thermoluminescent dosimeters (TLDs) were exposed at three different heights (106, 206, and 275 cm) above the concrete pad in a plane perpendicular to the reactor center-

line at 609.6 cm (20 ft) from the reactor center (in the same plane as the front face of the block house when it was added). At each height, four $\text{CaF}_2\text{:Mn}$ chips were exposed simultaneously in each iron capsule located in the vertical midplane of the configuration and 76.2 and 152.4 cm on each side of the midplane during each of three reactor runs. During these same runs, four chips were exposed every 4 ft along the centerline of the house (122 cm above the pad) beginning at the perpendicular plane 609.6 cm from the reactor center and extending out to 975 cm. The readouts from all the chips were converted to values of energy deposited within the iron capsule through the application of a previously determined calibration factor using ^{60}Co gamma rays as the source.

The results of the measurements, corrected only for the spectrum-weighted $1/f$ spectral correction factor for the ^{60}Co calibration source, are listed in Tables 15A and 15B. These values, expressed in terms of energy deposition per gram of iron, are not corrected for the neutron-induced dose nor for the $1/f$ factor for the experimentally generated gamma rays. These corrections are necessary when the TLD material (CaF_2) differs from the host medium (Fe).

Results from the TLD mapping in the vertical plane located 609.6 cm from the reactor centerline indicate a gradual decrease to 30% in the energy deposited in going from the centerline to 152.4 cm on each side centerline (from about 7.1×10^4 to 5.1×10^4 $\text{MeV g}^{-1} \text{min}^{-1} \text{kW}^{-1}$). These values represent the uncorrected gamma-ray source incident on the concrete wall of the house since this plane and the front face of the wall, when in position, were coincident. In going from 609.6 to 975 cm along the house axis (without the house present), the decrease in the energy absorption value approached a factor of three, from 6.52×10^4 to 2.39×10^4 $\text{MeV g}^{-1} \text{min}^{-1} \text{kW}^{-1}$.

6.2.2 Measurements in Concrete Block House

The locations of the TLDs exposed inside the four block house configurations were identified in Section 5 and in Fig. 9. Results from the exposures are listed in Table 18 and plotted in Fig. 18. Again, the values presented are uncorrected, as discussed earlier.

For the block house with a solid front wall, the results show very little difference in energy deposited at the three chip locations 15.2 cm beyond the front wall (positions 1, 2, and 3 in Fig. 18). Behind the pillar (points 7 and 8), the values dropped a factor of ten from those in front of the pillar, while near the back wall, where the chips were outside the shadow of the pillar, the values decreased by only a factor of three.

Opening the window in the front wall resulted in only a small increase (about 15%) in the energy absorption measured 61 cm off centerline 15.2 cm behind the front wall (positions 1 and 3); however, the energy deposited in the chips on centerline (positions 2 and 4) increased about a factor of five. The chips on centerline directly behind the center pillar (position 7) showed an increase of about 75%, while those located on centerline at 15.2 cm in front of the back wall (position 11) showed an increase of only

40%. The energy deposited at the two locations 15.2 cm in front of the back wall and 61 cm off centerline, which were outside the shadow of the pillar, increased about a factor of two.

Moving the pillar to the right side of the block house had only a small effect (maybe 4%) on the energy deposited in chips located in the front half of the house, but it increased the energy deposition in the chips on the centerline near the back wall (at position 11) by about a factor of 13. Likewise, the centerline chips 167.6 cm from the front wall (position 7), which had been previously protected by the center pillar but for this run looked directly at the source, indicated a factor of 20 increase in energy absorbed.

Placing the concrete wall at the middle of the house affected only those chips located behind it, decreasing the centerline value directly behind the wall (at position 7) about a factor of two and the centerline value just off the back wall by better than a factor of three. The fact that these ratios are not constant is believed to be attributable to the differences in the location of the chips with reference to the new wall. The wall attenuated both neutrons and gamma rays, which caused a similar loss of energy at both chip locations, but the wall also acted as a new source of gamma rays from neutron absorption and scattering (as well as gamma-ray scattering) and the location of this new source made a greater contribution to the chips directly behind the wall than it did to chips nearly 2 m away. The center wall also inhibited scattering from the side walls, whose contributions were more beneficial to the chips near the back wall.

The center wall had little effect on the chips behind the pillar located near the back wall (at position 12), causing maybe a 25% reduction, but for the chips at a similar position on the opposite side of the centerline (at position 10), the wall caused a factor of three reduction, as it did for the chips on the centerline.

7. ANALYSIS OF EXPERIMENTAL ERRORS

The errors associated with the measurements are due to: (1) uncertainties in the sizes and locations of voids (cracks) between the concrete bricks that formed the house wall; (2) uncertainties in the positions of the detectors and in their count rate statistics and calibrations; (3) uncertainties in the reactor power determinations; and (4) the effects of the exposure of the SM, the concrete pad, and the block house to the weather. Of these, the uncertainty due to exposure to the weather would be the most difficult to estimate. Changes in the moisture content in the graphite and the concrete would affect the number of neutrons transmitted to the detector. Precautions were taken to minimize this effect by covering both the SM and the block house with a plastic tarpaulin. This procedure was considered satisfactory for the SM, where count rates (without the block house present) obtained at the start of the experiment were essentially repeated at the end of the experiment. However, coverage with the tarpaulin was limited to the upper portion of the block house since the unevenness of the concrete pad permitted water to collect in isolated areas both inside and outside the house. During a rain and for some period afterwards (depending on amount of sunshine) the blocks in the lower rows of the walls would absorb and retain some moisture. The effect this moisture had on the flux reaching the detector was estimated to be less than 10%.

The double row of blocks forming the house walls were not mortared but were overlapped to minimize streaming. A visual inspection indicated no significant voids; the blocks appeared to be closely fitted and should have reasonably simulated a solid wall for this experiment.

The error associated with the Bonner ball measurements arising from calibration, counting statistics, and detector positioning should not exceed 5%.

The TSR-II power level for each measurement was determined from the output of two fission chambers located in the reactor shield along the midplane of the reactor. The responses of these chambers to the reactor source were monitored prior to the experiment through the use of gold foils and found to agree, within several percent, with the established reactor power values. These detectors were calibrated on a daily basis using a ^{252}Cf source, with the calibration values lying within about a 6% spread ($\pm 3\%$ of an average value). During any one detector traverse in a given day, the variation in the reactor power indicated by the monitor outputs was at most only a few percent; however, during the several months the experiment was being performed, the monitors indicated variations of about $\pm 5\%$. Thus, the uncertainty in the reactor power determination was assumed to be $\pm 5\%$.

8. CONCLUSION

Neutrons scattered back from the center pillar contributed about 25% of the count rate of the bare detector located on the block house centerline 61 cm beyond the front wall. For the 10-in. Bonner ball, the contribution was about 10%. With the concrete pillar moved to the right side of centerline and the center wall added, the contribution at the same location was about 20% for the bare detector and about 5% for the 10-in. ball. For the same two detectors located on centerline 61 cm in front of the back wall (no center wall), moving the pillar to the right side increased the bare detector count rate about a factor of two but increased the 10-in. ball count rate by a factor of ten.

Traverses at 61 cm in front of the back wall showed peaks in the count rates of different magnitudes between the pillar and the side walls when the pillar was positioned on centerline and the window was open in the front wall. These differences are due to misalignment of the window and pillar with respect to the reactor centerline.

Converting the solid front wall into a wall with a window increased the gamma-ray intensity on centerline in front of the pillar (positions 2 and 4, see Fig. 9) about a factor of five, but added only about 15% to the TLD readings 61 cm each side of centerline (positions 1 and 3). Moving the pillar to the right added, at most, a 5% contribution from backscattering to the TLDs directly in front of it (position 5), while it decreased the energy deposited in other chips in the front half of the house by similar amounts.

Establishing a window in the front wall increased the energy deposition in the TLDs in the back half of the room from about 70% directly behind the pillar on centerline to better than factors of two at locations on each side the pillar. Moving the pillar to the right side increased the values on centerline about a factor of 20 (at both positions 7 and 11), while it decreased the values behind the pillar (at position 12) nearly a factor of three. The addition of the center wall reduced the energy deposition in chips directly behind the wall (at position 7) by more than a factor of two and in chips next to the back wall (at position 11) by a factor of three. This difference in reduction was attributed to the generation of a new gamma-ray source from neutron capture in the added center wall adjacent to the TLDs at position 7 (but nearly 2 m from position 11) and to the removal of some of the gamma rays previously scattered to position 11 from the side wall before the center wall was added.

REFERENCES

1. R. E. Maerker, L. R. Williams, F. R. Mynatt, and N. M. Greene, *Response Functions for Bonner Ball Neutron Detectors*, ORNL/TM-3451 (June 18, 1971).
2. C. E. Burgart and M. B. Emmett, *Monte Carlo Calculations of the Response Functions of Bonner Ball Neutron Detectors*, ORNL/TM-3739 (April 3, 1972).
3. D. T. Ingersoll, private communication.

ACKNOWLEDGEMENTS

The author is grateful for the assistance of Dr. D. T. Ingersoll and W. A. Rhoades in the formulation of the Experimental Program Plan. Special thanks go to L. S. Abbott and A. C. Alford for their efforts in the editing and preparation of this report.

APPENDIX A**PROGRAM PLAN FOR THE THREE-DIMENSIONAL OAK RIDGE TRANSPORT
CALCULATIONAL METHODS VERIFICATION EXPERIMENT****I. Spectrum Modifier**

A. Spectrum Modifier (SM) (22.2 cm radial blanket + 10.2 cm borated polyethylene + 15.2 cm graphite)

1. Bare, Cd-covered, 5-, and 10-in. Bonner ball measurements:

- a. Horizontal midplane traverses at 30 cm beyond SM (traverses lie 207 cm above concrete pad)
- b. Horizontal traverses at several heights in a plane perpendicular to the SM centerline at 20 feet (609.6 cm) from reactor center, between 152.4 cm each side centerline.
 - i. At 91, 205, 275 cm above concrete pad (foreground only)
 - ii. At 122 cm above concrete pad (background only)
- c. Axial traverses along block house (to be) centerline, 85 cm below SM centerline (122 cm above pad) between 609.6 and 975.4 cm (20 to 32 feet), as measured on SM centerline, from vertical axis of reactor.

2. TLD measurements:

- a. Along horizontal lines in a plane perpendicular to SM centerline 609.6 cm from reactor center.
 - i. 106, 206, 275 cm above concrete pad at 0, 76.2, and 152.4 cm each side of the configuration centerline.
- b. Along block house (to be) centerline, 122 cm above concrete pad, at points 609.6, 762, 853.4, and 975.4 cm from reactor center as measured along SM centerline.

II. Concrete block wall building perpendicular to configuration centerline (front face 609.6 cm from reactor center as measured along SM centerline)

A. Spectrum Modifier + Concrete building + central concrete pillar + concrete window in front wall.

1. Bare, Cd-covered, 5-, and 10-in. Bonner ball measurements: (Foreground and Background)

- a. Horizontal traverses at 61 cm beyond front concrete wall at 122 cm above concrete pad.
- b. Horizontal traverses at 61 cm in front of back wall at 122 cm above concrete pad.

2. TLD measurements (Foreground and Background)

- a. On centerline and 61 cm each side centerline in horizontal plane at 15.2 cm back of front wall and 15.2 cm in front of back wall.
- b. On centerline and 61 cm right of centerline at 76.2 and 167.6 cm beyond front wall.

- c. At 30.5 and 213.4 cm above concrete pad on a vertical line through centerline at 167.6 cm beyond front wall.
- B. Spectrum modifier + concrete building + central concrete pillar + window void in front wall.
1. Bare, Cd-covered, 5-, and 10-in. Bonner ball measurements: (Foreground and Background)
 - a. Horizontal traverses at 61 cm beyond front concrete wall at 122 cm above concrete pad.
 - b. Horizontal traverses at 61 cm in front of back wall at 122 cm above concrete pad.
 2. TLD measurements (Foreground and Background):
 - a. On centerline and 61 cm each side centerline in horizontal plane at 15.2 cm back of front wall and 15.2 cm in front of back wall.
 - b. On centerline and 61 cm right of centerline at 76.2 and 167.6 cm beyond front wall.
 - c. At 30.5 and 213.4 cm above concrete pad on a vertical line through centerline at 167.6 cm beyond front wall.
- C. Spectrum modifier + concrete building + pillar at side of building + window void in front wall.
1. Bare, Cd-covered 5-, and 10-in. Bonner ball measurements:
 - a. Horizontal traverses at 61 cm beyond front concrete wall at 122 cm above concrete pad.
 - b. Horizontal traverses at 61 cm in front of back wall at 122 cm above concrete pad.
 2. TLD measurements (Foreground and Background):
 - a. On centerline and 61 cm each side centerline in horizontal plane at 15.2 cm back of front wall and 15.2 cm in front of back wall.
 - b. On centerline and 61 cm right of centerline at 76.2 and 167.6 cm beyond front wall.
- D. Spectrum modifier + concrete building + pillar at side of building + window void in front wall + central wall.
1. Bare, Cd-covered, 5-, and 10-in. Bonner ball measurements: (Foreground and Background)
 - a. Horizontal traverses at 61 cm beyond front concrete wall at 122 cm above concrete pad.
 - b. Horizontal traverses at 61 cm in front of back wall at 122 cm above concrete pad.
 2. TLD measurements (Foreground and Background):
 - a. On centerline and 61 cm each side centerline in horizontal plane at 15.2 cm back of front wall and 15.2 cm in front of back wall.
 - b. On centerline and 61 cm right of centerline at 76.2 and 167.6 cm beyond front wall.

APPENDIX B. TABLES OF DATA**List of Tables**

Table 1.	Composition of small concrete blocks (15.2 cm on a side and 30.5 cm long)
Table 2A.	Composition of large concrete blocks (61.0 cm on a side and 30.5 cm thick)
Table 2B.	Composition of concrete slabs in the ceiling (152.5 cm wide and 30.5 cm thick)
Table 3.	Chemical analysis of iron frame inside block house
Table 4.	Composition of UO ₂ radial blanket
Table 5.	Analysis of Na in radial blanket
Table 6.	Analysis of aluminum used in UO ₂ cladding
Table 7.	Composition of borated polyethylene slabs
Table 8.	Analysis for impurities in the graphite slabs
Table 9.	Bonner ball traverses 30 cm beyond spectrum modifier (Item I A)
Table 10.	Bonner ball traverses 20 feet from the vertical axis of the reactor and 275 cm above concrete pad (Item I A)
Table 11.	Bonner ball traverses 20 feet from the vertical axis of the reactor and 205 cm above concrete pad (Item I A)
Table 12.	Bonner ball traverses 20 feet from the vertical axis of the reactor and 91 cm above concrete pad (Item I A)
Table 13.	Bonner ball traverses within vertical midplane of reactor beam 122 cm above concrete pad (Item I A)
Table 14.	Bonner ball traverses 20 feet from the vertical axis of the reactor, 122 cm above concrete pad: background measurements with 61 cm LiH behind SM (Item I A)
Table 15A.	TLD measurements along horizontal lines 20 ft from the vertical axis of the reactor and 106, 206, and 275 cm above concrete pad (Item I A)
Table 15B.	TLD measurements within vertical midplane of reactor beam and 122 cm above concrete pad
Table 16.	Bonner ball traverses 61 cm beyond front wall of block house and 122 cm above concrete pad (Item II A)
Table 17.	Bonner ball traverses 61 cm in front of rear wall of block house and 122 cm above concrete pad (Item II A)
Table 18.	TLD measurements at various locations inside concrete block house (Items II A, B, C, D)
Table 19.	Bonner ball traverses 61 cm beyond front wall of block house and 122 cm above concrete pad (Item II B)
Table 20.	Bonner ball traverses 61 cm in front of rear wall of block house and 122 cm above concrete pad (Item II B)

- Table 21. Bonner ball traverses 61 cm beyond front wall of block house and 122 cm above concrete pad (Item II C)
- Table 22. Bonner ball traverses 61 cm in front of rear wall of block house and 122 cm above concrete pad (Item II C)
- Table 23. Bonner ball traverses 61 cm beyond front wall of block house and 122 cm above concrete pad (Item II D)
- Table 24. Bonner ball traverses at 61 cm in front of rear wall of block house and 122 cm above concrete pad (Item II D)

Table 1. Composition of small concrete blocks^a
(15.2 cm on a side by 30.5 cm long)

Element	wt. %
C	10.36
O	49.03
Ca	38.05
Fe	0.37
Si	0.78
Mg	0.23
S	0.17
P	0.04
Na	0.03
K	0.04
H	0.42
R ^b	0.47

^a $\rho = 2.39$ g/cc.

^bR is an unspecified mix of Al, Ti, Cr, and possibly other traces of metals.

Table 2A. Composition of large concrete blocks^a
(61 cm on a side and 30.5 cm thick)

Element	wt. %
CO ₃	41.9
Ca	27.4
SiO ₂	18.1
H ₂ O	4.0
Mg	3.66
O ₂	1.4
Al ₂ O ₃	2.2
Fe ₂ O ₃	0.60
SO ₃	0.32
P ₂ O ₅	0.035
K	0.30

^a $\rho = 3.14$ to 3.18 g/cc.

Table 2B. Composition of concrete slabs in the ceiling^a
(152.5 cm wide and 30.5 cm thick)

Element	wt. %
SiO ₂	9.17
CaO	34.18
Al ₂ O ₃	2.02
Fe ₂ O ₃	1.00
SO ₃	0.52
Na ₂ O	0.24
K ₂ O	0.58
P ₂ O ₅	0.06
LOI	38.54
R ₂ O ₃ ^b	3.02
CO ₂	37.0
H ₂ O (Free)	1.14
H ₂ O (Bound)	2.60
MgO	14.11

^a $\rho = 2.68$ g/cc.

^bR₂O₃ is an unspecified mix of Ti, Al, Cr, P, and possibly other traces of metals.

Table 3. Chemical analysis of iron frame inside block house

Element	wt. %
C	0.20
Co	0.0084
Cr	0.126
Fe	99.2
Mg	0.0051
Mn	0.5050
N	0.0056
Ni	0.121
O	0.0171
V	0.0170

Table 4. Composition of UO₂ radial blanket

Element	vol. %	Density (g/cc)
UO ₂ (pellets)	64.6 ^a	10.28
Al (8001)	11.2	2.8
Na	23.2	0.92
Void	1.0	-

U isotopic composition (%)			
Isotope, %			
²³⁴ U	0.0053	²³⁶ U	-
²³⁵ U	0.713	²³⁸ U	99.28

Metallic impurities in UO ₂ (ppm)					
Al	<20	Cu	1	Na	<20
B	<1	F	<2	Ni	<10
Be	<2	Fe	<20	Pb	<4
Bi	<2	H ₂ O	2.1	Si	<20
C	<10	Li	<1	Sn	<2
Ca	<20	Mg	<10	Ta	<25
Cd	<0.5	Mn	<4	Tu	<4
Cl	<3.3	Mo	<10	W	<25
Co	<2	N	54	Zr	<25
Cr	<10				

^a88.18 wt. %.**Table 5. Analysis of Na in radial blanket^a**

Element	wt. %
Na	99.7
Ca, Zn	0.3

^a $\rho = 0.92$ g/cc.

Table 6. Analysis of aluminum used in UO₂ cladding

Element	wt. %	ppm
Fe	0.59	
Ni	1.13	
B		<6
Be		<20
Cd		<20
Co		<20
Cr		<6
Cu		52.9
Li		6
Ng		3.04
Mn		11.2
Mö		<6
Pb		<20
Si		27.5
Sn		<60
Ta		<2000
Ti		65.5
V		44.2
W		<60
Zr		<20

Table 7. Composition of borated polyethylene slabs^{a,b}

Element	wt. %
Hydrogen	11.6
Boron	5.0
Carbon	61.2
Oxygen	22.2

^a $\rho = 0.94$ g/cc.

^bSupplied by vendor, Reactor Experiments, Inc.

Table 8. Analysis for impurities in the graphite slabs^a

Element	wt. %	Element	wt. %
Ag	<0.005	Mn	<0.001
Al	0.007	Mo	<0.001
Au	<0.005	Na	0.002
B	<0.001	Nb	<0.005
Ba	0.007	Ni	<0.001
Be	<0.0001	Pb	<0.002
Bi	<0.002	Pt	<0.005
Ca	0.07	Rb	<0.002
Cd	<0.005	Sb	<0.005
Co	<0.002	Si	0.01
Cr	<0.002	Sn	<0.002
Cs	<0.005	Sr	<0.001
Cu	<0.001	Ta	<0.005
Fe	0.02	Te	<0.01
Ga	<0.002	Ti	0.005
Ge	<0.002	V	<0.002
Hg	<0.005	W	<0.005
K	0.002	Zn	<0.005
Li	0.002	Zr	<0.005
Mg	0.001		

^a $\rho = 1.73 \text{ g/cc.}$ **Table 9. Bonner ball traverses 30 cm beyond spectrum modifier (Item I A)**

Distance from vertical midplane (cm)	Bonner ball count rates ($\text{s}^{-1} \text{W}^{-1}$)			
	Bare counter	Cd-covered counter	5-in.-diam ball	10-in.-diam ball
76.2 N	3.72 (1) ^a	3.61 (0)	1.23 (2)	6.52 (1)
60	4.95 (1)	5.53 (0)	1.92 (2)	1.08 (2)
45	6.06 (1)	7.50 (0)	2.68 (2)	1.51 (2)
30	7.25 (1)	9.34 (0)	3.42 (2)	1.96 (2)
15	8.05 (1)	1.07 (1)	3.84 (2)	2.28 (2)
0	8.46 (1)	1.13 (1)	4.08 (2)	2.37 (2)
15	8.27 (1)	1.09 (1)	4.02 (2)	2.34 (2)
30	7.53 (1)	9.70 (0)	3.50 (2)	2.06 (2)
45	6.45 (1)	7.91 (0)	2.82 (2)	1.63 (2)
60	5.31 (1)	6.03 (0)	2.09 (2)	1.20 (2)
76.2 S	4.21 (1)	4.24 (0)	1.38 (2)	7.61 (1)

^aRead: 3.72×10^1 .

Table 10. Bonner ball traverses 20 ft from the vertical axis of the reactor and 275 cm above concrete pad^a (Item I A)

Distance from vertical midplane (cm)	Bonner ball count rates ($s^{-1} W^{-1}$)			
	Bare counter	Cd-covered counter	5-in.-diam ball	10-in.-diam ball
111 N	2.53 (0) ^b	2.49 (-1)	8.56 (0)	5.24 (0)
90	2.57 (0)	2.55 (-1)	8.82 (0)	
81				5.54 (0)
60	2.64 (0)	2.64 (-1)	9.11 (0)	
51				5.72 (0)
30	2.68 (0)	2.69 (-1)	9.23 (0)	
21				5.81 (0)
0	2.71 (0)	2.69 (-1)	9.25 (0)	
9				5.80 (0)
30	2.64 (0)	2.64 (-1)	9.24 (0)	
39				5.75 (0)
60	2.63 (0)	2.63 (-1)	9.08 (0)	
69				5.62 (0)
90	2.58 (0)	2.55 (-1)	8.70 (0)	
99				5.31 (0)
117 S	2.47 (0)	2.44 (-1)	8.32 (0)	5.12 (0)

^aThe 20-ft distance corresponds to the location of the front face of the block house.

^bRead: 2.53×10^0 .

Table 11. Bonner ball traverses at 20 ft from the vertical axis of the reactor and 205 cm above concrete pad^a (Item I A)

Distance from vertical midplane (cm)	Bonner ball count rates ($s^{-1} W^{-1}$)			
	Bare counter	Cd-covered counter	5-in.-diam ball	10-in.-diam ball
111 N	2.79 (0) ^b	2.80 (-1)	9.23 (0)	5.75 (0)
90	2.89 (0)	2.82 (-1)	9.51 (0)	5.93 (0)
60	2.97 (0)	2.89 (-1)	9.86 (0)	6.20 (0)
30	2.99 (0)	2.96 (-1)	1.00 (1)	6.32 (0)
0	3.00 (0)	3.00 (-1)	9.95 (0)	6.18 (0)
	3.08 (0)	2.98 (-1)	1.02 (1)	6.42 (0)
30	3.01 (0)	2.97 (-1)	1.00 (1)	6.13 (0)
	3.06 (0)	2.96 (-1)	1.01 (1)	6.34 (0)
60	2.96 (0)	2.91 (-1)	9.85 (0)	6.18 (0)
	3.03 (0)	2.97 (-1)	1.00 (1)	6.05 (0)
90	2.86 (0)	2.82 (-1)	9.52 (0)	5.97 (0)
	2.93 (0)	2.86 (-1)	9.54 (0)	5.79 (0)
120	2.71 (0)	2.65 (-1)	8.85 (0)	5.62 (0)
	2.81 (0)	2.64 (-1)	9.02 (0)	5.43 (0)
150	2.64 (0)	2.53 (-1)	8.49 (0)	5.03 (0)
180	2.50 (0)	2.36 (-1)	7.90 (0)	4.63 (0)
193.8 S	2.43 (0)	2.33 (-1)	7.58 (0)	4.49 (0)

^aThe 20-ft distance corresponds to the front face of the block house and the 205-cm height approximates the horizontal midplane of the reactor beam (at 207 cm).

^bRead: 2.79×10^0 .

Table 12. Bonner ball traverses 20 ft from the vertical axis of the reactor and 91 cm above concrete pad^a (Item I A)

Distance from vertical midplane (cm)	Bonner ball count rates ($s^{-1} W^{-1}$)			
	Bare counter	Cd-covered counter	5-in.-diam ball	10-in.-diam ball
115.6 N		2.82 (-1) ^b		
115	2.96 (0)		9.16 (0)	5.34 (0)
90	3.01 (0)		9.52 (0)	5.52 (0)
85.6		2.89 (-1)		
60	3.12 (0)		9.82 (0)	5.80 (0)
55.6		2.95 (-1)		
30	3.16 (0)		9.87 (0)	5.91 (0)
25.6		2.93 (-1)		
0	3.15 (0)		9.92 (0)	5.94 (0)
4.4		2.93 (-1)		
30	3.17 (0)		9.89 (0)	5.92 (0)
34.4		2.93 (-1)		
60	3.10 (0)		9.85 (0)	5.88 (0)
64.4		2.97 (-1)		
90	3.06 (0)		9.49 (0)	5.63 (0)
94.4		2.82 (-1)		
113		2.70 (-1)		
117.3			9.08 (0)	5.33 (0)
117.8 S	2.91 (0)			

^aThe 20-ft distance corresponds to the location of the front face of the block house.

^bRead: 2.82×10^{-1} .

Table 13. Bonner ball traverses within vertical midplane of reactor beam 122 cm above concrete pad^a (Item I A)

Distance from reference point ^b (cm)	Bonner ball count rates (s ⁻¹ W ⁻¹)			
	Bare counter	Cd-covered counter	5-in.-diam ball	10-in.-diam ball
Foreground + Background				
0		2.98 (-1) ^c	1.02 (1)	5.99 (0)
7	3.12 (0)			
30	2.84 (0)	2.71 (-1)	9.11 (0)	5.37 (0)
60	2.58 (0)	2.46 (-1)	8.34 (0)	4.91 (0)
90	2.35 (0)	2.22 (-1)	7.62 (0)	4.54 (0)
120	2.14 (0)	2.03 (-1)	6.86 (0)	4.09 (0)
150	1.96 (0)	1.86 (-1)	6.35 (0)	3.78 (0)
180	1.80 (0)	1.68 (-1)	5.75 (0)	3.44 (0)
185		1.66 (-1)		
210	1.64 (0)	1.56 (-1)	5.30 (0)	3.19 (0)
240	1.51 (0)	1.43 (-1)	4.87 (0)	2.97 (0)
270	1.40 (0)	1.34 (-1)	4.54 (0)	2.76 (0)
300	1.30 (0)	1.25 (-1)	4.21 (0)	2.58 (0)
330	1.19 (0)	1.12 (-1)	3.85 (0)	2.39 (0)
360	1.10 (0)	1.06 (-1)	3.62 (0)	2.22 (0)
390	1.02 (0)	9.97 (-2)	3.36 (0)	2.10 (0)
Background Only^d				
0	2.42 (-1)	9.70 (-3)	2.42 (-1)	9.02 (-2)
360	1.02 (-1)	4.75 (-3)	1.08 (-1)	3.85 (-2)

^aThe 122-cm height corresponds to the horizontal midplane of the block house.

^bThe reference point (0) was 470 cm from the SM (20 ft from the vertical axis of the reactor) in a vertical plane corresponding to the front face of the block house.

^cRead: 2.98×10^{-1} .

^dBackground measurements made with 61 cm LiH placed directly behind SM.

Table 14. Bonner ball traverses 20 ft from the vertical axis of the reactor, 122 cm above concrete pad: background measurements with 61 cm LiH behind SM^a (Item I A)

Distance from vertical midplane (cm)	Bonner ball count rates (s ⁻¹ W ⁻¹)			
	Bare counter	Cd-covered counter	5-in.-diam ball	10-in.-diam ball
110 N	2.55 (-1) ^b	1.26 (-2)	2.89 (-1)	1.14 (-1)
80	2.69 (-1)	1.33 (-2)	3.52 (-1)	1.23 (-1)
50	2.50 (-1)	1.11 (-2)	2.62 (-1)	9.68 (-2)
20	2.41 (-1)	1.03 (-2)	2.47 (-1)	9.08 (-2)
0		9.70 (-3)	2.42 (-1)	9.02 (-2)
10	2.42 (-1)			
20			2.35 (-1)	8.71 (-2)
30		9.80 (-3)		
40	2.36 (-1)			
50			2.41 (-1)	8.65 (-2)
60		1.01 (-2)		
70	2.36 (-1)			
80	2.38 (-1)		2.58 (-1)	9.46 (-2)
90	2.37 (-1)	1.07 (-2)		
118		1.09 (-2)	2.60 (-1)	9.76 (-2)
120 S	2.34 (-1)			

^aThe 20-ft distance corresponds to the front face of the block house and the 122-cm height corresponds to its horizontal midplane.

^bRead: 2.55×10^{-1} .

Table 15A. TLD measurements along horizontal lines 20 ft from the vertical axis of the reactor^a and 106, 206, and 275 cm above concrete pad (Item I A)

Distance from vertical midplane ^b (cm)	Energy deposition ^c (MeV g ⁻¹ min ⁻¹ kW ⁻¹)		
	At 106 cm	At 206 cm	At 275 cm
152.4 N	5.19 (4) ^d	5.61 (4)	5.47 (4) ± 0.26
76.2 N	6.09 (4)	6.73 (4)	6.44 (4) ± 0.33
0	6.41 (4)	7.07 (4)	6.70 (4) ± 0.35
76.2 S	6.03 (4)	6.59 (4)	6.28 (4) ± 0.32
152.4 S	5.11 (4)	5.58 (4)	5.43 (4) ± 0.28

^aThe 20-ft distance corresponds to the front face of the block house.

^bSee TLD locations in Fig. 8.

^cNot corrected for neutron interactions in the chip or the spectrum-averaged $1/f$ factor for gamma rays generated during the experiment.

^dRead: 5.19×10^4 .

Table 15B. TLD measurements within vertical midplane of reactor beam and 122 cm above concrete pad^a

Distance from vertical axis of reactor ^b (cm)	Energy deposition ^c (MeV g ⁻¹ min ⁻¹ kW ⁻¹)
	122 cm
609.6 ^d	6.52 (4)
731.5	4.41 (4)
853.4	3.15 (4)
975.4	2.39 (4) ± 0.13

^aThe 122-cm height corresponds to the horizontal midplane of the block house.

^bSee TLD locations in Fig. 8.

^cNot corrected for neutron interactions in the chips or the spectrum-averaged $1/f$ factor for gamma rays generated during the experiment.

^dThis point (20 ft from the vertical axis of the reactor) corresponds to the front face of the block house.

Table 16. Bonner ball traverses 61 cm beyond front wall of block house and 122 cm above concrete pad^a (Item II A)

Distance from vertical midplane (cm)	Bonner ball count rates ($s^{-1} W^{-1}$)			
	Bare counter	Cd-covered counter	5-in.-diam ball	10-in.-diam ball
Foreground + Background				
91.4 N	1.46 (0) ^b	5.22 (-2)	1.32 (0)	6.07 (-1)
75	1.51 (0)		1.28 (0)	6.54 (-1)
60	1.61 (0)	5.07 (-2)	1.35 (0)	6.70 (-1)
45	1.67 (0)		1.35 (0)	6.90 (-1)
30	1.75 (0)	5.23 (-2)	1.37 (0)	7.22 (-1)
15	1.86 (0)		1.39 (0)	7.23 (-1)
0	1.84 (0)	5.37 (-2)	1.41 (0)	7.27 (-1)
15	1.85 (0)	5.21 (-2)	1.38 (0)	7.19 (-1)
30	1.71 (0)	5.13 (-2)	1.34 (0)	7.09 (-1)
45	1.67 (0)	4.95 (-2)	1.32 (0)	6.81 (-1)
60	1.55 (0)	4.92 (-2)	1.27 (0)	6.57 (-1)
75	1.50 (0)	4.86 (-2)	1.28 (0)	6.37 (-1)
91.4 S	1.44 (0)	4.99 (-2)	1.29 (0)	5.83 (-1)
Background Only^c				
91.4 N	5.63 (-2)	1.08 (-1)	3.27 (-2)	9.65 (-3)
60	4.75 (-2)		2.18 (-2)	
30	4.57 (-2)		1.91 (-2)	
0	4.65 (-2)	5.93 (-2)	1.87 (-2)	6.49 (-3)
30		6.06 (-2)		6.67 (-3)
60		6.69 (-2)		7.46 (-3)
91.4 S	5.51 (-2)	8.96 (-2)	3.04 (-2)	9.37 (-3)

^aThe 122-cm height corresponds to the horizontal midplane of the block house.

^bRead: 1.46×10^0 .

^cBackground measurements made with 61 cm LiH placed directly behind SM.

Table 17. Bonner ball traverses 61 cm in front of rear wall of block house and 122 cm above concrete pad^a (Item II A)

Distance from vertical midplane (cm)	Bonner ball count rates ($s^{-1} W^{-1}$)			
	Bare counter	Cd-covered counter	5-in.-diam ball	10-in.-diam ball
Foreground + Background				
91.4 N	6.65 (-1) ^b	2.30 (-2)	5.46 (-1)	2.34 (-1)
75	6.71 (-1)	2.06 (-2)	4.91 (-1)	2.27 (-1)
60	6.77 (-1)	1.88 (-2)	4.57 (-1)	2.12 (-1)
45	6.69 (-1)	1.82 (-2)	4.28 (-1)	1.93 (-1)
30	6.70 (-1)	1.72 (-2)	3.93 (-1)	1.62 (-1)
15	6.55 (-1)	1.66 (-2)	3.61 (-1)	1.45 (-1)
0	6.57 (-1)	1.63 (-2)	3.69 (-1)	1.43 (-1)
15	6.70 (-1)	1.67 (-2)	3.83 (-1)	1.52 (-1)
30	6.73 (-1)	1.77 (-2)	4.16 (-1)	1.78 (-1)
45	6.75 (-1)	1.82 (-2)	4.42 (-1)	2.04 (-1)
60	6.75 (-1)	1.93 (-2)	4.66 (-1)	2.20 (-1)
75	6.73 (-1)	2.06 (-2)	5.05 (-1)	2.35 (-1)
91.4 S	6.58 (-1)	2.24 (-2)	5.33 (-1)	2.34 (-1)
Background Only^c				
91.4 N	3.35 (-2)	1.00 (-3)	1.87 (-2)	5.23 (-3)
60	2.63 (-2)		1.17 (-2)	3.37 (-3)
30	2.41 (-2)	5.48 (-4)	9.51 (-3)	2.81 (-3)
0	2.32 (-2)	5.14 (-4)	9.30 (-3)	2.65 (-3)
30	2.45 (-2)	5.72 (-4)	1.02 (-2)	3.05 (-3)
60		6.66 (-4)		
91.4 S	3.18 (-2)	9.09 (-4)	1.74 (-2)	5.03 (-3)

^aThe 122-cm height corresponds to the horizontal midplane of the block house.

^bRead: 6.65×10^{-1} .

^cBackground measurements made with 61 cm LiH placed directly behind SM.

Table 18. TLD measurements at various locations inside concrete block house^{a,b} (Items II A, B, C, D)

TLD position	Energy deposition (MeV g ⁻¹ min ⁻¹ kW ⁻¹) ^c			
	Conf. A	Conf. B	Conf. C	Conf. D
1	1.22 (4) ^d	1.38 (4)	1.33 (4) ± 0.07	1.46 (4) ± 0.08
2	1.30 (4)	6.66 (4) ± 0.37	6.73 (4)	6.86 (4) ± 0.35
3	1.23 (4)	1.38 (4)	1.36 (4)	1.44 (4) ± 0.08
4	1.08 (4) ± 0.06	5.86 (4)	5.41 (4)	5.60 (4) ± 0.29
5	9.13 (3)	1.05 (4)	1.11 (4) ± 0.06	1.15 (4)
6	9.76 (2) ± 0.55	1.64 (3)		
7	1.14 (3)	1.94 (3) ± 0.12	3.84 (4)	1.72 (4)
8	1.14 (3) ± 0.07	1.68 (3)		
9	5.57 (3)	8.07 (3)	2.36 (3) ± 0.12	1.15 (3)
10	3.66 (3) ± 0.22	9.73 (3)	1.23 (4)	4.61 (3)
11	1.57 (3)	2.21 (3) ± 0.13	2.80 (4)	8.10 (3)
12	3.63 (3)	8.21 (3)	2.81 (3) ± 0.15	2.13 (3) ± 0.13

^aSee Fig. 9 for TLD positions (i.e., in horizontal midplane of block house) except positions 6 and 8, which were 91.4 cm below and above horizontal midplane, respectively.

^bBlock house configurations:

- A: SM + blockhouse + concrete window + center pillar.
- B: SM + blockhouse + open window + center pillar.
- C: SM + blockhouse + open window + offset pillar.
- D: SM + blockhouse + open window + offset pillar + center block wall.

^cNot corrected for neutron interactions in the chips or for spectrum-averaged $1/f$ spectral correction for gamma rays generated during experiment.

^dRead: 1.22×10^4 .

Table 19. Bonner ball traverses 61 cm beyond front wall of block house and 122 cm above concrete pad^a (Item II B)

Distance from vertical midplane (cm)	Bonner ball count rates ($s^{-1} W^{-1}$)			
	Bare counter	Cd-covered counter	5-in.-diam ball	10-in.-diam ball
Foreground + Background				
91.4 N	2.22 (0) ^b	8.43 (-2)	2.04 (0)	8.59 (-1)
75	2.38 (0)	9.17 (-2)	2.27 (0)	9.76 (-1)
60	2.62 (0)	1.03 (-1)	2.57 (0)	1.09 (0)
45	2.94 (0)	1.23 (-1)	3.14 (0)	1.56 (0)
37.5		1.68 (-1)		
30	3.93 (0)	2.31 (-1)	7.16 (0)	4.04 (0)
22.5	4.20 (0)			
15	4.32 (0)	2.64 (-1)	8.17 (0)	4.84 (0)
7.5				4.91
0	4.42 (0)	2.67 (-1)	8.34 (0)	4.94 (0)
15	4.24 (0)	2.55 (-1)	8.01 (0)	4.85 (0)
22.5				4.56 (0)
28			6.99(0)	
30	3.67 (0)	2.13 (-1)		3.62 (0)
37.5	3.11 (0)	1.47 (-1)		2.24 (0)
45	2.79 (0)	1.15 (-1)	2.89 (0)	1.37 (0)
60	2.53 (0)	9.77 (-2)	2.42 (0)	1.07 (0)
75	2.32 (0)	8.93 (-2)		9.41 (-1)
79			2.14 (0)	
91.4 S	2.09 (0)	8.20 (-2)	1.92 (0)	8.25 (-1)
Background Only^c				
91.4 N	1.03 (-1)		8.28 (-2)	
60	1.11 (-1)		8.65 (-2)	
30			1.61 (-1)	
0	2.27 (-1)		1.91 (-1)	
30	1.74 (-1)			
45			9.94 (-2)	
60	1.07 (-1)			
75 S			7.90 (-2)	

^aThe 122-cm height corresponds to the horizontal midplane of the block house.

^bRead: 2.22×10^0 .

^cBackground measurements made with 61 cm LiH placed directly behind SM.

Table 20. Bonner ball traverses 61 cm in front of rear wall of block house and 122 cm above concrete pad^a (Item II B)

Distance from vertical midplane (cd)	Bonner ball count rates ($s^{-1} W^{-1}$)			
	Bare counter	Cd-covered counter	5-in.-diam ball	10-in.-diam ball
Foreground + Background				
91.4 N	9.68 (-1) ^b	3.47 (-2)	8.20 (-1)	3.16 (-1)
75	1.06 (0)	3.68 (-2)	8.90 (-1)	3.89 (-1)
67.5		3.99 (-2)		
60	1.13 (0)	4.44 (-2)	1.25 (0)	6.45 (-1)
52.5		4.60 (-2)	1.37 (0)	7.56 (-1)
45	1.12 (0)	4.25 (-2)	1.21 (0)	6.67 (-1)
37.5		3.33 (-2)		
30	1.05 (0)	3.05 (-2)	6.80 (-1)	2.75 (-1)
15	1.04 (0)	2.94 (-2)	6.62 (-1)	2.34 (-1)
0	1.04 (0)	3.01 (-2)	6.62 (-1)	2.41 (-1)
15	1.06 (0)	3.05 (-2)	6.89 (-1)	2.48 (-1)
22.5			7.41 (-1)	
30	1.12 (0)	3.94 (-2)	1.12 (0)	5.82 (-1)
37.5		4.85 (-2)	1.53 (0)	8.95 (-1)
45	1.19 (0)	5.31 (-2)	1.66 (0)	9.74 (-1)
52.5		5.01 (-2)	1.46 (0)	8.30 (-1)
60	1.12 (0)	4.41 (-2)	1.20 (0)	6.33 (-1)
67.5		3.97 (-2)		
75	1.06 (0)	3.69 (-2)	9.04 (-1)	3.91 (-1)
91.4 S	9.62 (-1)	3.44 (-2)	8.09 (-1)	3.22 (-1)
Background Only^c				
91.4 N	6.15 (-2)		3.46 (-2)	1.01 (-2)
60	5.10 (-2)		2.74 (-2)	9.55 (-3)
30				5.20 (-3)
0	4.39 (-2)		1.74 (-2)	4.80 (-3)
45	5.02 (-2)		2.87 (-2)	1.03 (-2)
75 S	5.67 (-2)		2.86 (-2)	8.90 (-3)

^aThe 122-cm height corresponds to the horizontal midplane of the block house.

^bRead: 9.68×10^{-1} .

^cBackground measurements made with 61 cm LiH placed directly behind SM.

Table 21. Bonner ball traverses 61 cm beyond front wall of block house and 122 cm above concrete pad^a (Item II C)

Distance from vertical midplane (cm)	Bonner ball count rates ($s^{-1} W^{-1}$)			
	Bare counter	Cd-covered counter	5-in.-diam ball	10-in.-diam ball
91.4 N	2.07 (0) ^b	7.96 (-2)	1.89 (0)	7.94 (-1)
75	2.29 (0)	8.49 (-2)	2.05 (0)	8.81 (-1)
60	2.50 (0)	9.45 (-2)	2.29 (0)	9.71 (-1)
45	2.70 (0)	1.05 (-1)	2.71 (0)	1.33 (0)
37.5	2.98 (0)	1.44 (-1)	4.17 (0)	2.31 (0)
30	3.34 (0)	2.00 (-1)	6.37 (0)	3.63 (0)
22.5				4.27 (0)
15	3.47 (0)	2.19 (-1)	7.24 (0)	4.42 (0)
0	3.40 (0)	2.18 (-1)	7.21 (0)	4.40 (0)
7.5				4.37 (0)
15	3.30 (0)	2.10 (-1)	7.08 (0)	4.30 (0)
22.5	3.17 (0)			
30	2.96 (0)	1.79 (-1)	5.62 (0)	3.21 (0)
37.5		1.17 (-1)	3.40 (0)	
45	2.36 (0)	9.35 (-2)	2.34 (0)	1.11 (0)
60	2.19 (0)	8.40 (-2)	2.10 (0)	9.15 (-1)
75	2.08 (0)	7.88 (-2)	1.95 (0)	8.46 (-1)
91.4 S	1.91 (0)	7.41 (-2)	1.81 (0)	7.50 (-1)

^aThe 122-cm height corresponds to the horizontal midplane of the block house.

^bRead: 2.07×10^0 .

Table 22. Bonner ball traverses 61 cm in front of rear wall of block house and 122 cm above concrete pad^a (Item II C)

Distance from vertical midplane (cm)	Bonner ball count rates ($s^{-1} W^{-1}$)			
	Bare counter	Cd-covered counter	5-in.-diam ball	10-in.-diam ball
91.4 N	1.10 (0) ^b	3.98 (-2)	9.02 (-1)	3.21 (-1)
75	1.20 (0)	4.14 (-2)	9.29 (-1)	3.34 (-1)
60	1.29 (0)	4.30 (-2)	1.00 (0)	3.76 (-1)
45	1.38 (0)	4.79 (-2)	1.11 (0)	4.34 (-1)
37.5				6.07 (-1)
30	1.58 (0)	6.87 (-2)	1.73 (0)	1.12 (0)
22.5		9.69 (-2)	2.92 (0)	1.86 (0)
15	1.89 (0)	1.08 (-1)	3.59 (0)	2.34 (0)
7.5			3.80 (0)	2.42 (0)
0	1.97 (0)	1.14 (-1)	3.83 (0)	2.45 (0)
7.5			3.84 (0)	
15	1.95 (0)	1.10 (-1)	3.80 (0)	2.43 (0)
22.5		1.07 (-1)	3.66 (0)	
30	1.90 (0)	1.03 (-1)	3.47 (0)	2.14 (0)
37.5	1.85 (0)	9.57 (-2)		
45	1.78 (0)	8.63 (-2)	2.75 (0)	1.54 (0)
60	1.63 (0)	6.90 (-2)	1.99 (0)	9.27 (-1)
75	1.49 (0)	5.83 (-2)	1.47 (0)	6.04 (-1)
91.4 S	1.32 (0)	5.16 (-2)	1.26 (0)	4.95 (-1)

^aThe 122-cm height corresponds to the horizontal midplane of the block house.

^bRead: 1.10×10^0 .

Table 23. Bonner ball traverses 61 cm beyond front wall of block house and 122 cm above concrete pad^a (Item II D)

Distance from vertical midplane (cm)	Bonner ball count rates ($s^{-1} W^{-1}$)			
	Bare counter	Cd-covered counter	5-in.-diam ball	10-in.-diam ball
Foreground + Background				
91.4 N	2.36 (0) ^b	8.78 (-2)	2.06 (0)	8.27 (-1)
75	2.63 (0)	9.61 (-2)	2.26 (0)	9.33 (-1)
60	2.89 (0)	1.07 (-1)	2.52 (0)	1.03 (0)
45	3.20 (0)	1.22 (-1)	3.02 (0)	1.40 (0)
37.5	3.55 (0)	1.63 (-1)	4.46 (0)	2.38 (0)
30	3.99 (0)	2.22 (-1)	6.74 (0)	3.68 (0)
22.5	4.21 (0)	2.46 (-1)	7.70 (0)	4.43 (0)
15	4.25 (0)	2.50 (-1)	7.87 (0)	4.56 (0)
0	4.22 (0)	2.49 (-1)	7.91 (0)	4.57 (0)
15	4.13 (0)	2.46 (-1)	7.75 (0)	4.55 (0)
22.5	4.05 (0)	2.36 (-1)	7.51 (0)	4.36 (0)
30	3.88 (0)	2.13 (-1)	6.65 (0)	3.55 (0)
45	3.15 (0)	1.26 (-1)	3.14 (0)	1.43 (0)
60	2.98 (0)	1.14 (-1)	2.76 (0)	1.13 (0)
75	2.81 (0)	1.06 (-1)	2.55 (0)	1.02 (0)
91.4 S	2.54 (0)	9.81 (-2)	2.32 (0)	9.16 (-1)
Background Only^c				
91.4 N	1.05 (-1)	2.98 (-3)	5.67 (-2)	1.61 (-2)
60	1.15 (-1)	3.04 (-3)	5.99 (-2)	1.81 (-2)
30	1.59 (-1)	4.85 (-3)	1.14 (-1)	4.39 (-2)
0	1.89 (-1)	5.84 (-3)	1.42 (-1)	5.57 (-2)
30	1.55 (-1)	4.61 (-3)	1.10 (-1)	4.00 (-2)
60	1.12 (-1)	2.96 (-3)	5.75 (-2)	1.70 (-2)
91.4 S	1.01 (-1)	2.61 (-3)	5.11 (-2)	1.51 (-2)

^aThe 122-cm height corresponds to the horizontal midplane of the block house.

^bRead: 2.36×10^0 .

^cBackground measurements made with 61 cm LiH placed directly behind SM.

Table 24. Bonner ball traverses at 61 cm in front of rear wall of block house and 122 cm above concrete pad^a (Item II D)

Distance from vertical midplane (cm)	Bonner ball count rates ($s^{-1} W^{-1}$)			
	Bare counter	Cd-covered counter	5-in.-diam ball	10-in.-diam ball
Foreground + Background				
91.4 N	7.22 (-1) ^b	2.77 (-2)	6.66 (-1)	2.57 (-1)
75	7.43 (-1)	2.63 (-2)	6.40 (-1)	2.62 (-1)
60	7.74 (-1)	2.62 (-2)	6.54 (-1)	2.86 (-1)
45	8.01 (-1)	2.68 (-2)	6.90 (-1)	3.15 (-1)
30	8.29 (-1)	2.87 (-2)	7.53 (-1)	3.97 (-1)
22.5	8.40 (-1)	2.96 (-2)	8.39 (-1)	4.85 (-1)
15	8.58 (-1)	3.00 (-2)	8.56 (-1)	5.29 (-1)
0	8.82 (-1)	3.08 (-2)	8.89 (-1)	5.78 (-1)
15	8.85 (-1)	3.11 (-2)	8.98 (-1)	5.75 (-1)
22.5				5.69 (-1)
30	8.86 (-1)	3.11 (-2)	8.91 (-1)	5.43 (-1)
45	8.70 (-1)	3.04 (-2)	8.52 (-1)	4.67 (-1)
60	8.46 (-1)	3.07 (-2)	8.03 (-1)	3.92 (-1)
75	8.00 (-1)	2.98 (-2)	7.62 (-1)	3.43 (-1)
91.4 S	7.74 (-1)	3.04 (-2)	7.67 (-1)	
Background Only^c				
91.4 N	3.78 (-2)	1.13 (-3)	2.34 (-2)	6.59 (-3)
60	3.01 (-2)	8.10 (-4)	1.56 (-2)	4.49 (-3)
30	2.97 (-2)	7.60 (-4)	1.39 (-2)	4.77 (-3)
0	3.01 (-2)	7.90 (-4)	1.47 (-2)	5.70 (-3)
30	3.04 (-2)	7.96 (-4)	1.52 (-2)	5.66 (-3)
60	3.14 (-2)	8.43 (-4)	1.60 (-2)	5.33 (-3)
91.4 S	3.54 (-2)	1.08 (-3)	1.98 (-2)	6.02 (-3)

^aThe 122-cm height corresponds to the vertical midplane of the block house.

^bRead: 7.22×10^{-1} .

^cBackground measurements made with 61 cm LiH placed directly behind SM.

APPENDIX C. LIST OF FIGURES

List of Figures

- Fig. 1. Photograph of TORT experimental configuration.
- Fig. 2. Schematic of SM and concrete block house (Items IA, IIA).
- Fig. 3. Sketch of the radial blanket assembly and details of UO₂ fuel pins (top view).
- Fig. 4. Schematic of SM and concrete block house (Item II B).
- Fig. 5. Photograph of concrete block house with window in front wall (Item II B).
- Fig. 6. Schematic of SM and concrete block house (Item II C).
- Fig. 7. Schematic of SM and concrete block house (Item II D).
- Fig. 8. Schematic of main frame and TLD exposure locations relative to main frame of block house (Items II A, B, C, D).
- Fig. 9. Plan view of Bonner ball traverse locations and TLD positions.
- Fig. 10. Count rate profiles for bare BF₃ counter along horizontal traverses 61 cm beyond front wall of block house (Items II A, B, C, D).
- Fig. 11. Count rate profiles for Cd-covered BF₃ counter along horizontal traverses 61 cm beyond front wall of block house (Items II A, B, C, D).
- Fig. 12. Count rate profiles for 5-in. Bonner ball along horizontal traverse 61 cm beyond front wall of block house (Items II A, B, C, D).
- Fig. 13. Count rate profiles for 10-in. Bonner ball along horizontal traverses 61 cm beyond front wall of block house (Items II A, B, C, D).
- Fig. 14. Count rate profiles for bare BF₃ detector along horizontal traverses 61 cm in front of rear wall of block house (Items II A, B, C, D).
- Fig. 15. Count rate profiles for Cd-covered BF₃ detector along horizontal traverses 61 cm in front of rear wall of block house (Items II A, B, C, D).
- Fig. 16. Count rate profiles for 5-in. Bonner ball along horizontal traverses 61 cm in front of rear wall of block house (Items II A, B, C, D).
- Fig. 17. Count rate profiles for 10-in. Bonner ball along horizontal traverses 61 cm in front of rear wall of block house (Items II A, B, C, D).
- Fig. 18. Gamma-ray energy deposition profiles for TLDs inside concrete block house (Items II A, B, C, D).



Fig. 1. Photograph of TORT experimental configuration.

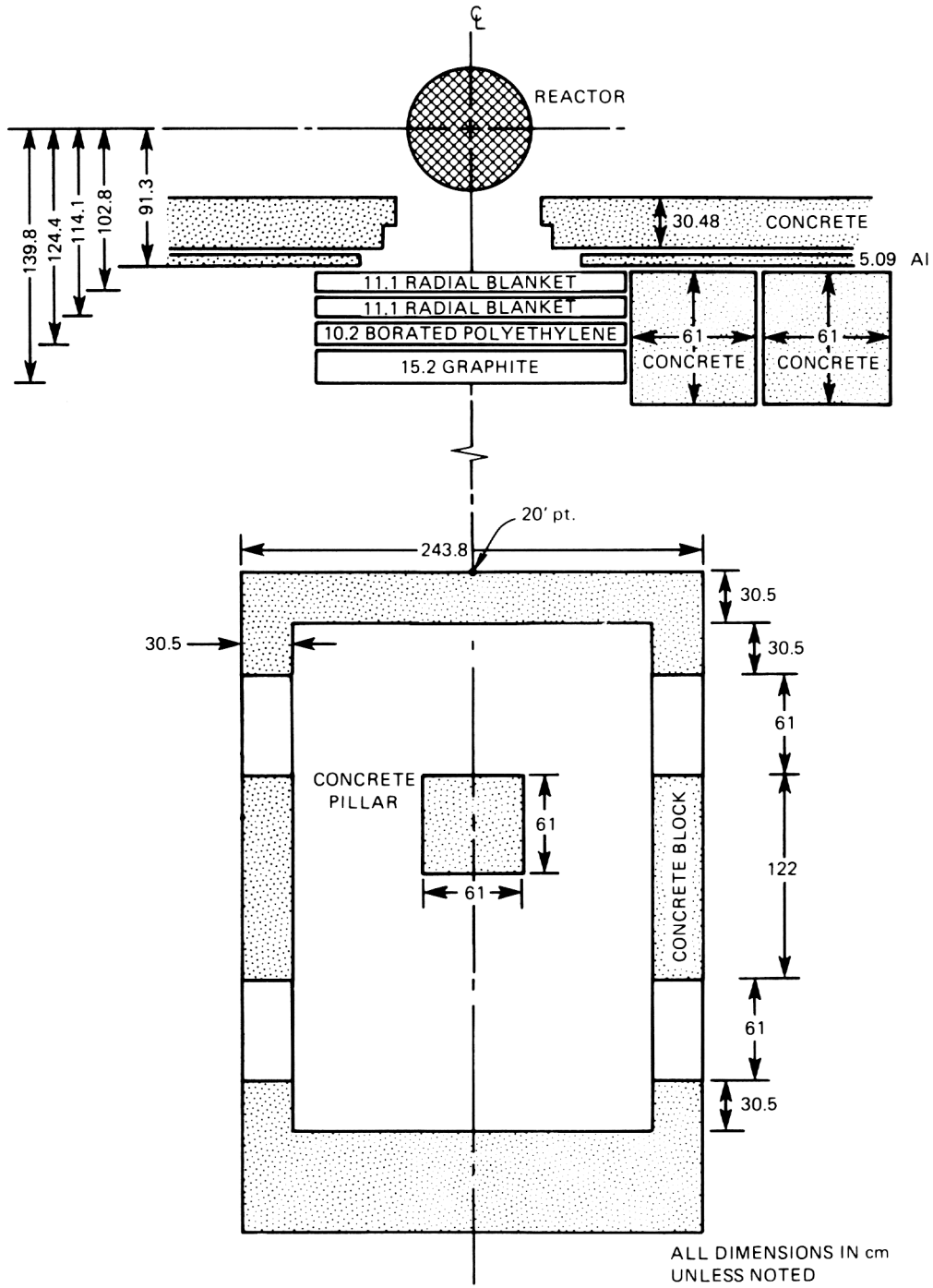
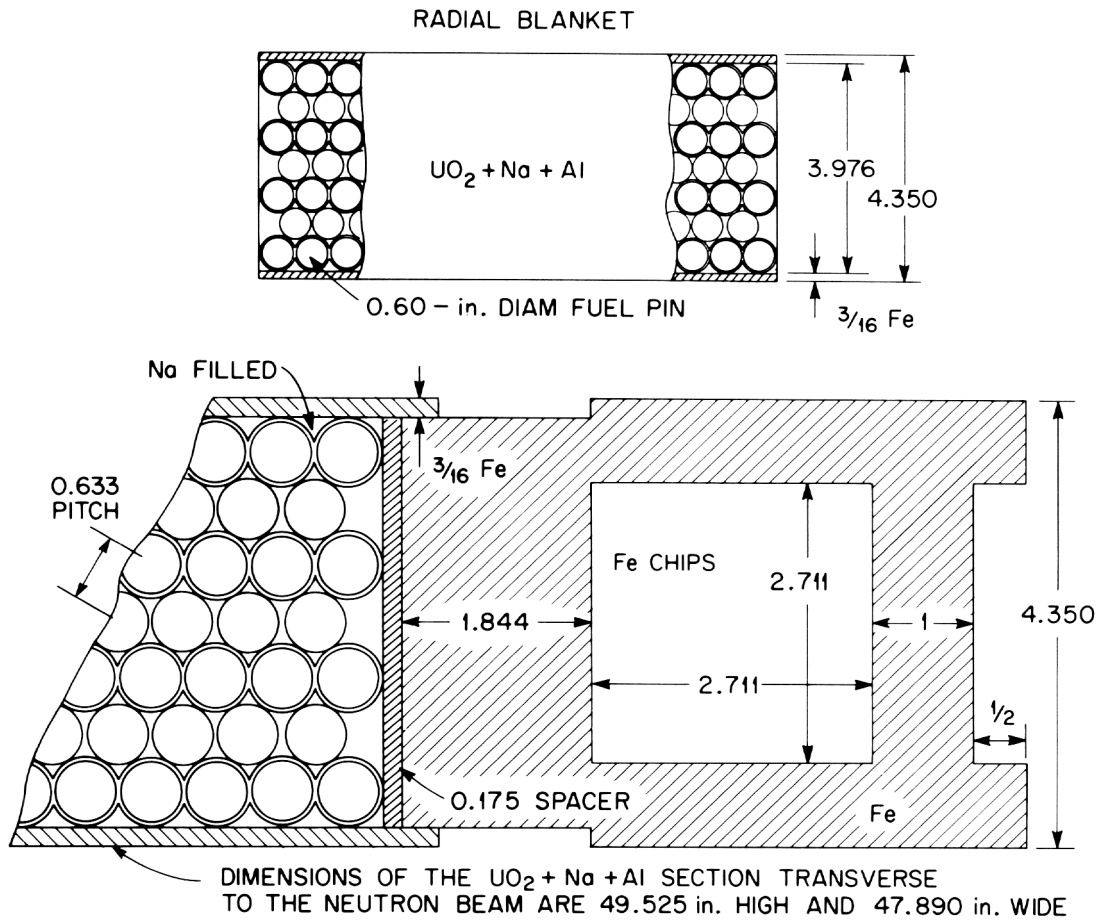
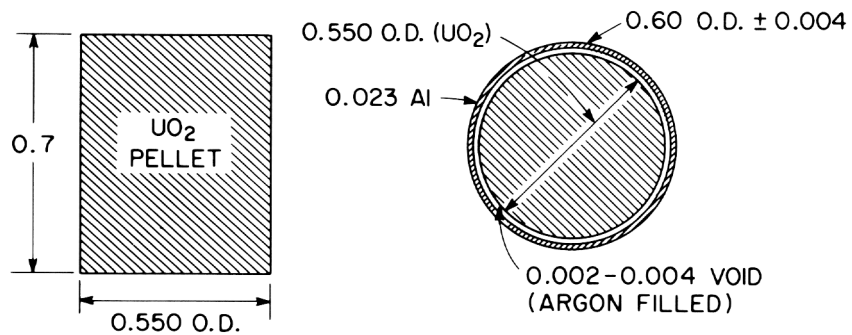


Fig. 2. Schematic of SM and concrete block house (Items IA, IIA).



THEORETICAL DENSITY = 10.96 g/cc
ACTUAL DENSITY (0.94 THEO.) = 10.28 g/cc



DIMENSIONS ARE IN INCHES

Fig. 3. Sketch of the radial blanket assembly and details of UO_2 fuel pins (top view).

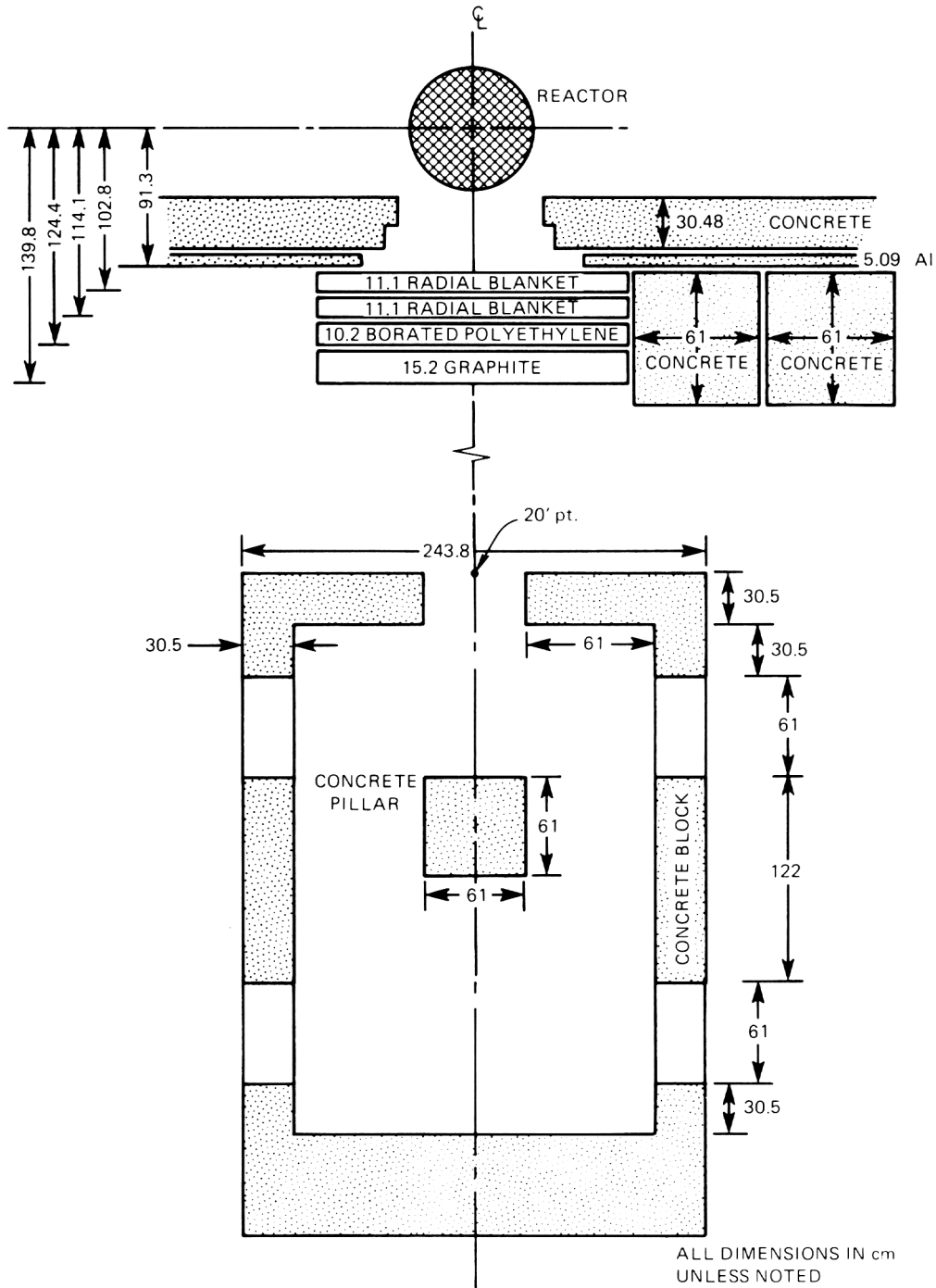


Fig. 4. Schematic of SM and concrete block house (Item II B).



Fig. 5. Photograph of concrete block house with window in front wall (Item II B).

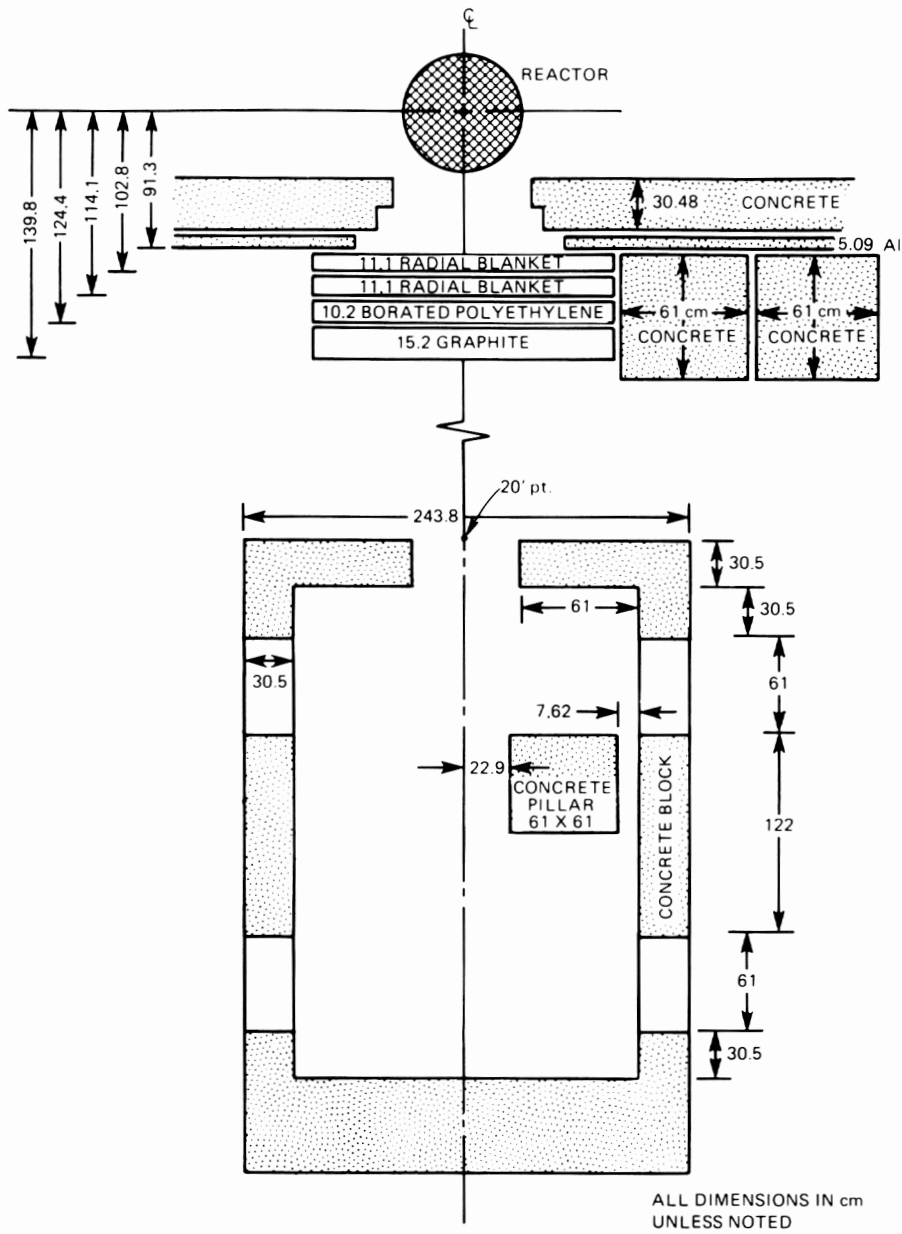


Fig. 6. Schematic of SM and concrete block house (Item II C).

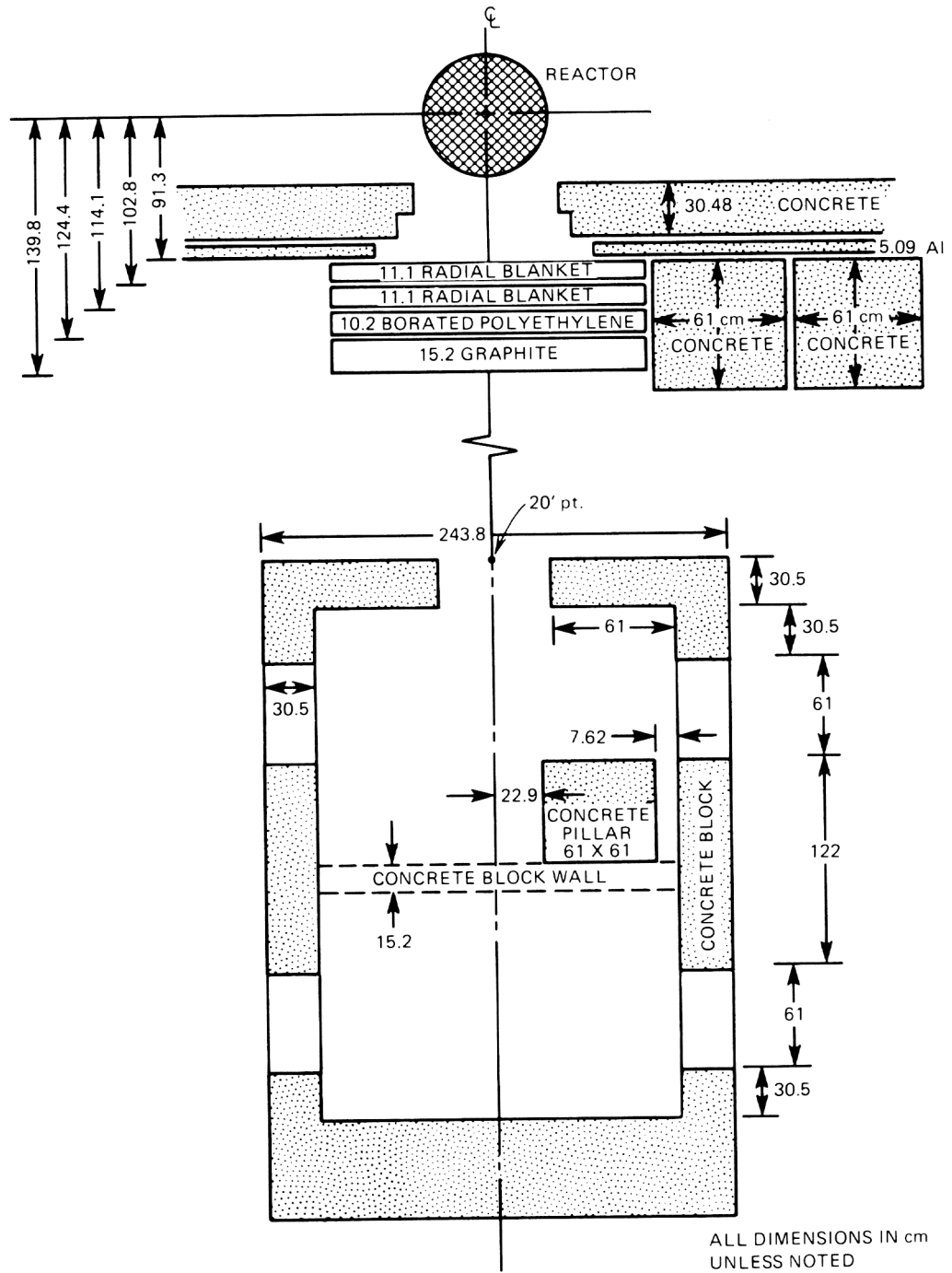


Fig. 7. Schematic of SM and concrete block house (Item II D).

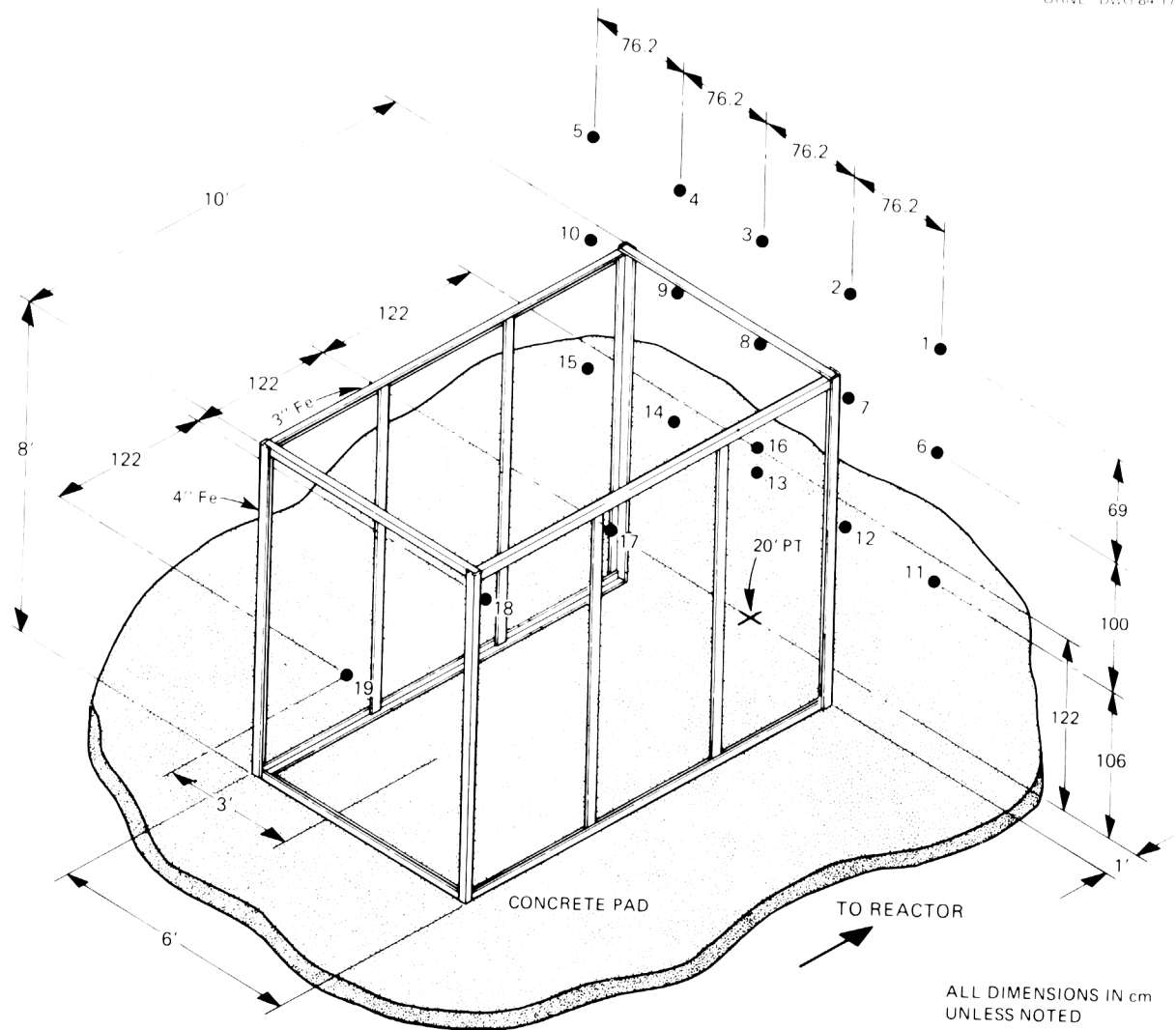
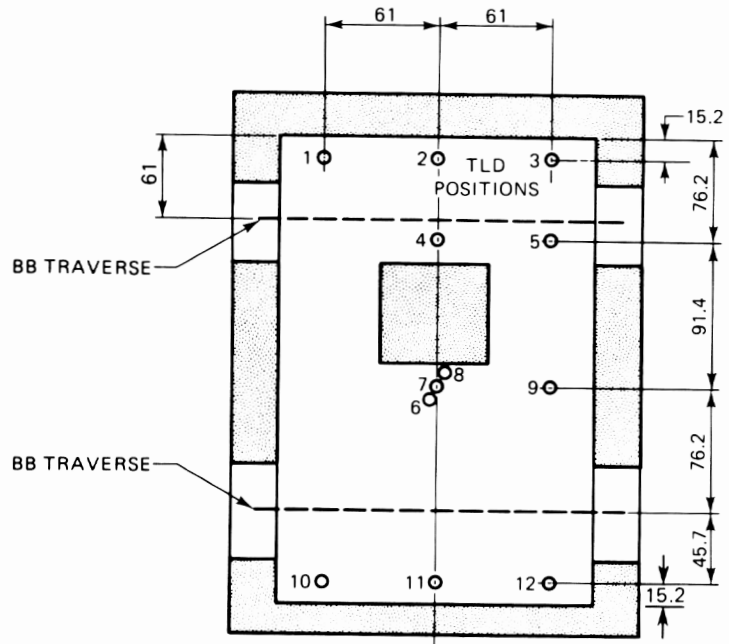
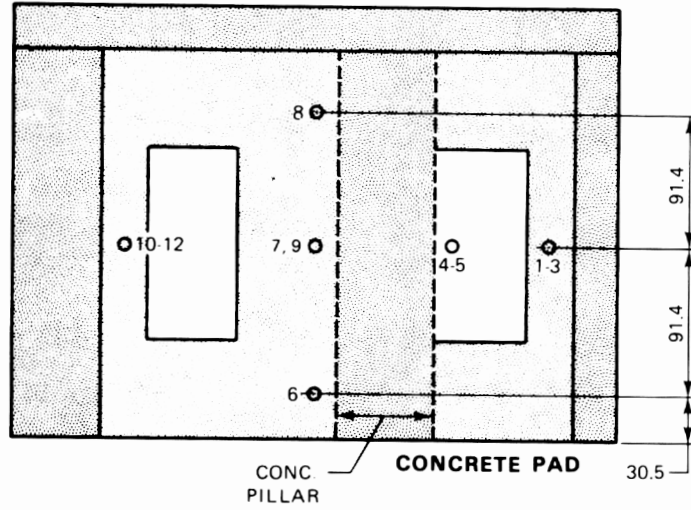


Fig. 8. Schematic of main frame and TLD exposure locations relative to main frame of block house (Items II A, B, C, D).



TOP VIEW

ALL DIMENSIONS ARE IN CENTIMETERS



SIDE VIEW

Fig. 9. Plan view of Bonner ball traverse locations and TLD positions.

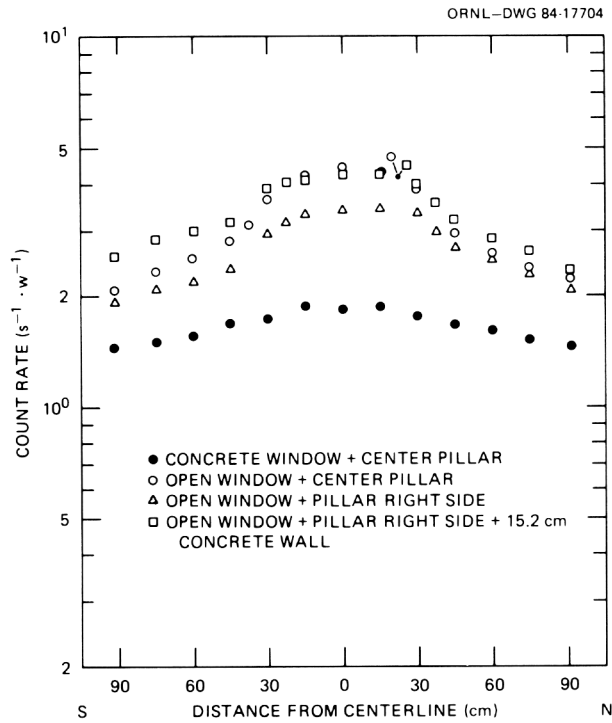


Fig. 10. Count rate profiles for bare BF_3 counter along horizontal traverses 61 cm beyond front wall of block house (Items II A, B, C, D).

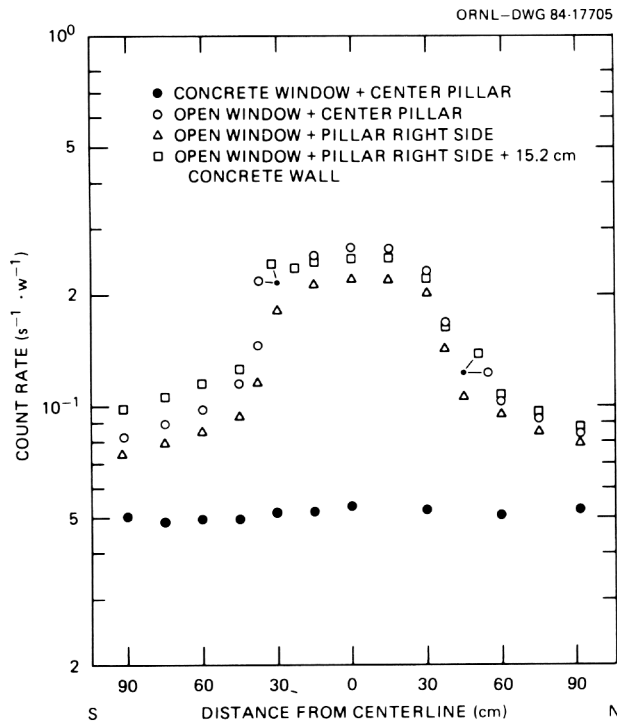


Fig. 11. Count rate profiles for Cd-covered BF_3 counter along horizontal traverses 61 cm beyond front wall of block house (Items II A, B, C, D).

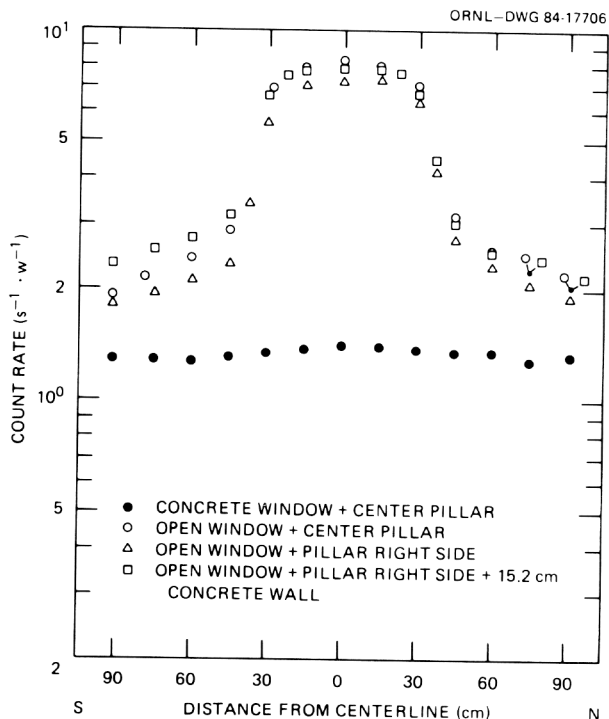


Fig. 12. Count rate profiles for 5-in. Bonner ball along horizontal traverse 61 cm beyond front wall of block house (Items II A, B, C, D).

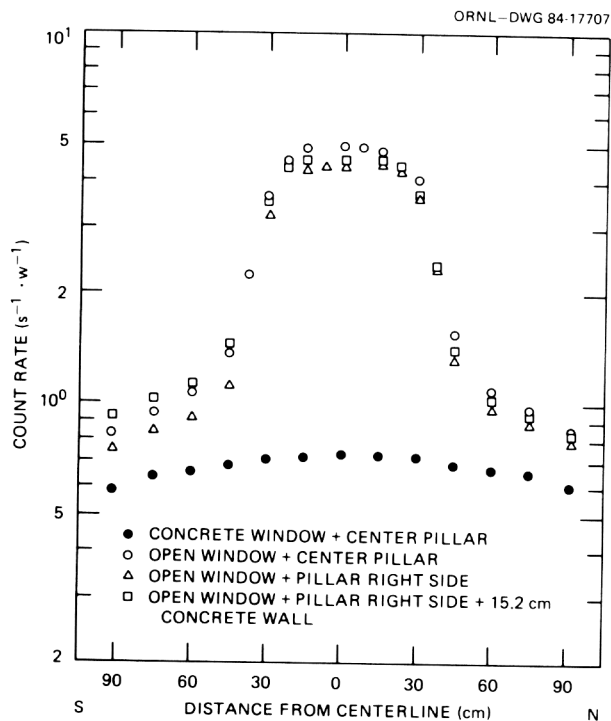


Fig. 13. Count rate profiles for 10-in. Bonner ball along horizontal traverses 61 cm beyond front wall of block house (Items II A, B, C, D).

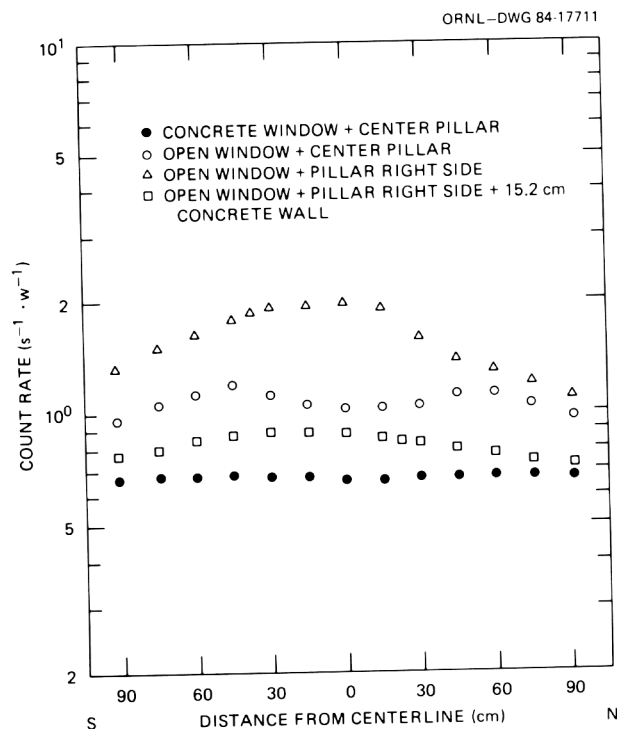


Fig. 14. Count rate profiles for bare BF_3 detector along horizontal traverses 61 cm in front of rear wall of block house (Items II A, B, C, D).

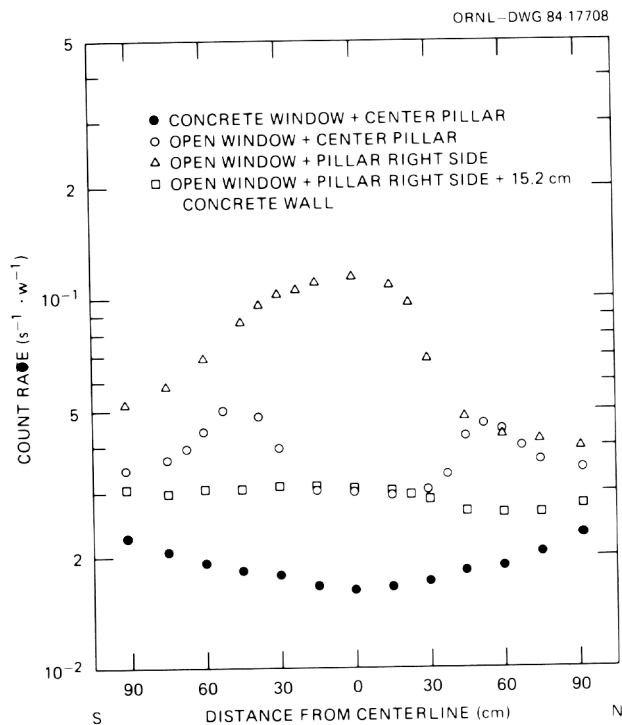


Fig. 15. Count rate profiles for Cd-covered BF_3 detector along horizontal traverses 61 cm in front of rear wall of block house (Items II A, B, C, D).

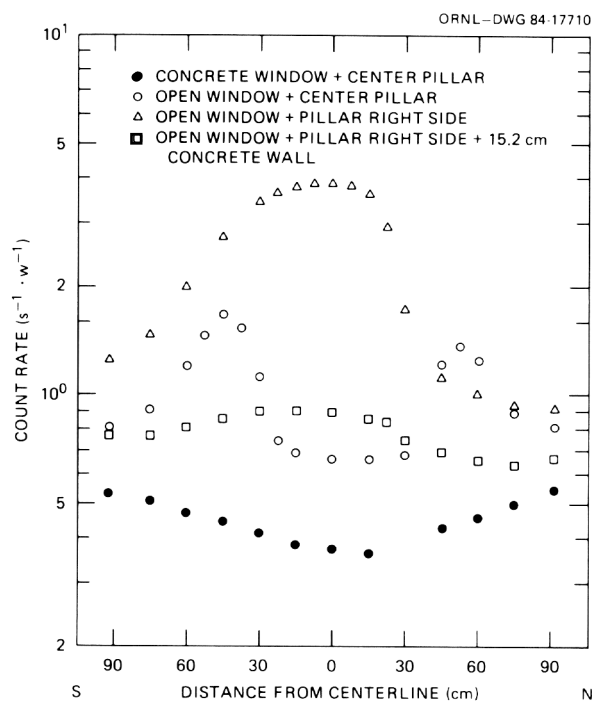


Fig. 16. Count rate profiles for 5-in. Bonner ball along horizontal traverses 61 cm in front of rear wall of block house (Items II A, B, C, D).

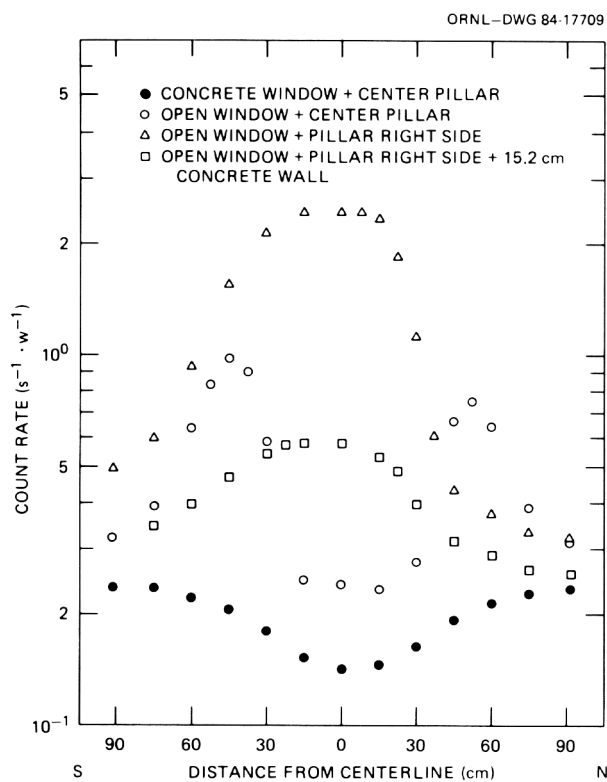


Fig. 17. Count rate profiles for 10-in. Bonner ball along horizontal traverses 61 cm in front of rear wall of block house (Items II A, B, C, D).

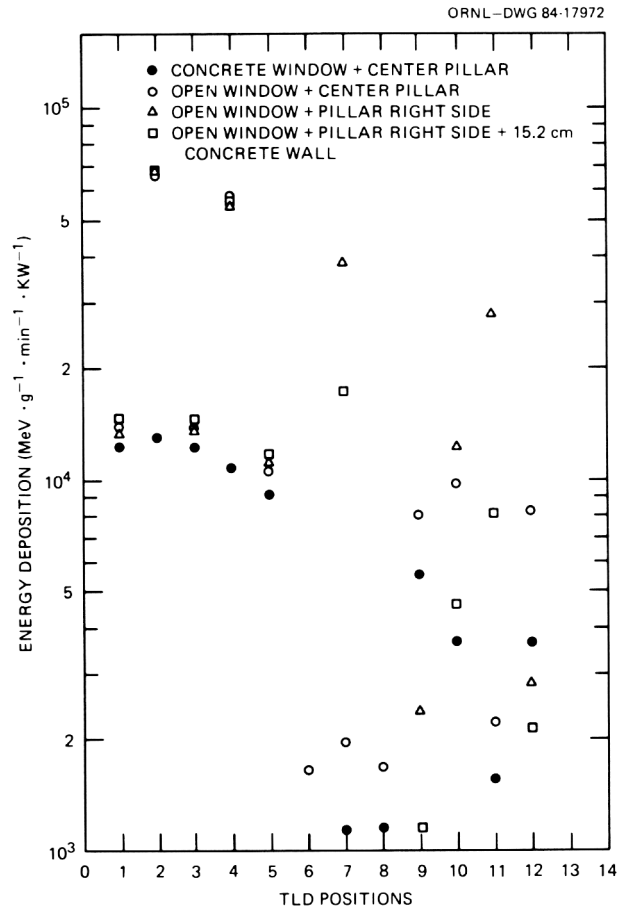


Fig. 18. Gamma-ray energy deposition profiles for TLDs inside concrete block house (Items II A, B, C, D).

INTERNAL DISTRIBUTION

1-5.	L. S. Abbott	30.	R. W. Peelle
6.	D. G. Cacuci	31.	W. A. Rhoades
7.	R. L. Childs	32.	R. W. Roussin
8.	J. C. Cleveland	33.	C. O. Slater
9.	S. N. Cramer	34.	J. S. Tang
10.	W. W. Engle, Jr.	35.	D. R. Vondy
11.	L. B. Holland	36.	A. Zucker
12.	F. J. Homan	37.	P. W. Dickson, Jr. (Consultant)
13.	J. L. Hull	38.	G. H. Golub (Consultant)
14.	D. T. Ingersoll	39.	D. Steiner (Consultant)
15.	J. O. Johnson	40-41.	Central Research Library
16.	R. A. Lillie	42.	Y-12 Technical Library
17.	R. E. Maerker		Document Reference Section
18-22.	F. C. Maienschein	43-44.	Laboratory Records Department
23.	J. J. Manning	45.	Laboratory Records ORNL, RC
24-28.	F. J. Muckenthaler	46.	ORNL Patent Office
29.	J. V. Pace	47.	EPIC
		48-52.	EPMD Reports Office

EXTERNAL DISTRIBUTION

- 53. Office of the Assistant Manager for Energy Research and Development, DOE-ORO, Oak Ridge, TN 37830, Attention: S. W. Ahrends/M. Rohr
- 54-80. Technical Information Center
- 81-152. DNA Radiation Transport Distribution